subunits belong either to the same TRP subfamily or to a different subfamily, giving rise to a wide variety of channels [101].

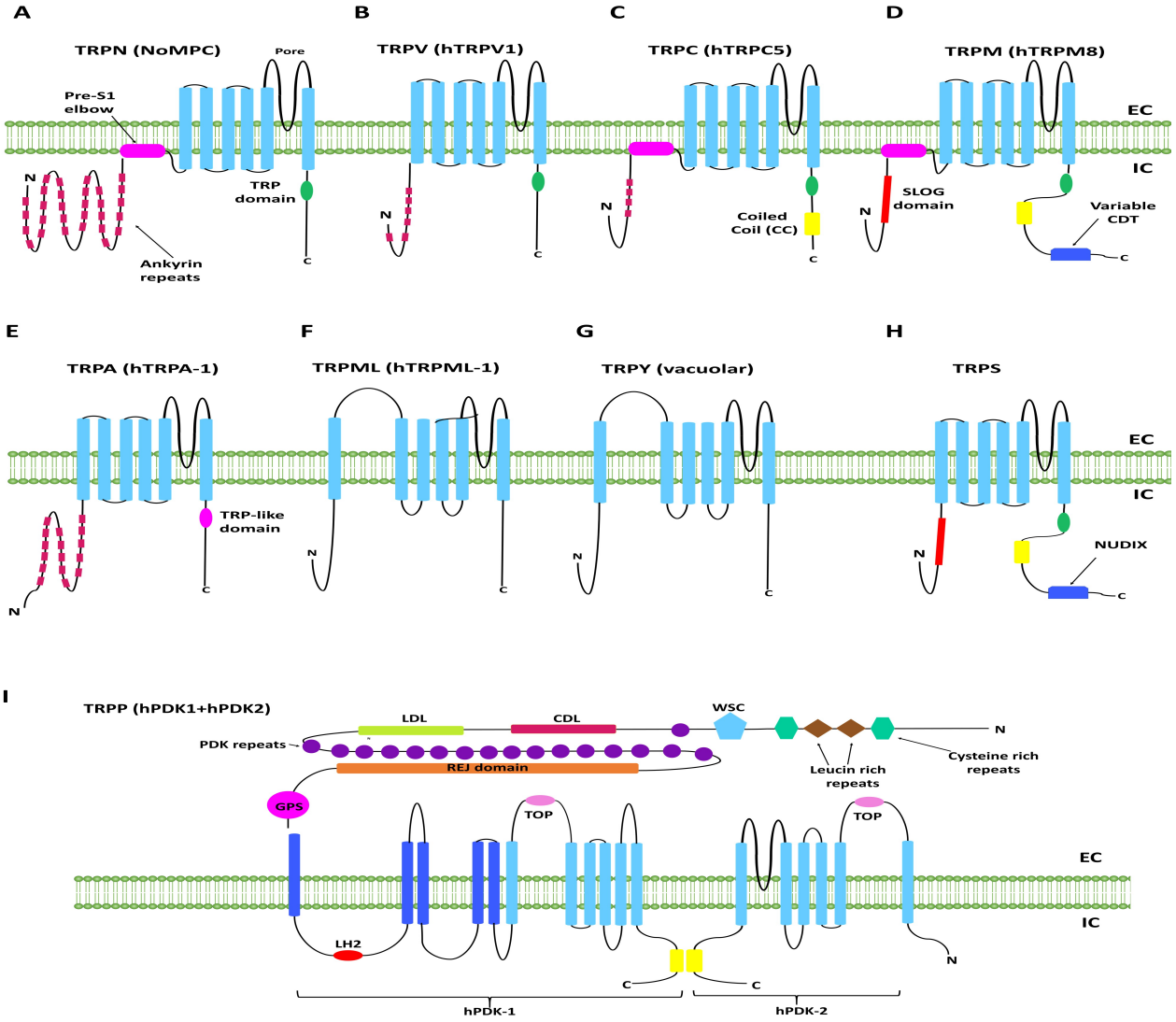

Figure 4. Transient Receptor Potential (TRP) channels diagram. (**A**) TRPN (NoMPC). TRPN channels have six transmembrane domains with 29 highly-conserved ankyrin repeats (adapted from [99]). (**B**) TRPV channels. Representative diagram of human TRPV1 channels. In addition to the six transmembrane domains, TRPV channels have six ankyrin repeats (adapted from [99]). (**C**) TRPC channels. Representative diagram of TRPC channels (e.g., hTRPC5). In addition to the six transmembrane domain, TRPC5 channels have four ankyrin repeats, a PRE-S1 domain, as well as a coiled-coil domain (adapted from [99,103]). (**D**) TRPM channels. Representative structure of the TRPM channels (e.g., hTRPM8). The channels have six transmembrane domain, a SLOG domain, a TRP domain, a coiled-coil domain, and a Variable C-terminal domain. The Variable C-terminal domain could encode an alpha-kinase domain or a nudix-hydrolase domain. (adapted from [99,104]). (**E**) TRPA channels. Structure of human TRPA-1 channels (e.g., hTRPA1, adapted from [99,105]). TRPA channels have a high number of ankyrin. The number of ankyrin domains is variable between species and between TRPA1 channels of the same species. (**F**) TRPM-L channels. (adapted from [99]). (**G**) Structure of the vacuolar TRPY channels (adapted from [99,106]). (**H**) TRPS channels. The structure of TRPS channels needs further investigation. Their structure is similar to that of TRPML channels, and they are expressed among mollusks, nematodes, tardigrades, myriapods, and chelicerates [99]. Their structure includes a SLOG domain, a TRP domain, and a nudix-Hydrolase domain. (adapted from [99,107]). (**I**) TRPP channels. Structure of the TRPP channels (e.g., hPDK-1 and hPDK-2). PDK-1 and PDK-2 are expressed together and form a protein complex (adapted from [108]).

Channels from almost every family have been shown to be involved in mechanosensation [1,101,109]. The only two families whose members are not involved in mechanosensation are the TRPML and the TRPS [99,110]. The complete list of mechanosensitive TRP channels expressed in neuronal cells is reported in Table 2. In the following, we discuss the current knowledge of the role of TRP channels in mechanosensation and their gating mechanisms, with some specific examples.

TRP channels are involved in many mechanosensory processes including, auditory transduction [111–114], gentle touch sensation [113–118], regulation of blood pressure [119,120], proprioception [121–123], nociception [124–126], shear stress detection [127], and also photomechanical responses [128].

The mechanosensory ability of TRP channels and their gating mechanism by force are still debated. Based on how they react to mechanical stimuli, mechanosensitive TRP channels can be divided into two main categories: the mechanically-gated (MG) channels and the mechanically sensitive channels [129]. The first class includes the force sensors themselves that are directly activated by the stimulus [130,131], while the others are activated by second messengers whose release is triggered by the activation of the primary force sensor [128–134].

Many works have reported force-evoked currents in many types of TRP channels, including TRPN [102,115,122], TRPV [135–138], TRPC [139–145], TRPM [127,146,147], TRPP [116,148,149], and TRPA [150,151]. These currents are evoked by different kinds of mechanical stimuli including membrane stretch, pressure application, and osmotic changes. However, in most cases, the mechanosensitivity of the channels and their gating mechanism are still debated and poorly understood. Recently, Nikolaev et al. [131] have demonstrated that 11 mammalian TRP channels, previously reported to originate stretch-evoked currents [102,115,116,122,124,127,135–151], do not respond to negative pressure application when heterologously expressed in HEK293T cells or in liposomes [131]. These results are confirmed by other works that have revised the intrinsic stretch activation of TRPC1 and TRPC6 [152], TRPV4 [153], TRPM4 [154], and TRPP (PDK2) channels [132,133]. Overall, these findings suggest that further investigation is needed to clarify the specific mechanisms of mechanical gating in TRP channels. The gating may depend not only on the applied stimulus but also on the specific cellular environment and on the lipidic composition of the membrane [130,131], raising the possibility that many TRPs are downstream a primary mechanoreceptor, rather than being mechanoreceptors themselves [129–131].

A particular example of indirect mechanical activation of TRP channels is given by the photomechanically activated TRPs in *Drosophila*. In this scenario, the phospholipase C (PLC) pathway activated by the G-protein signaling results in the conversion of phosphatidylinositol4, 5-biphosphate (PIP_2) into diacylglycerol (DAG). DAG occupies significantly lower space in the membrane than PIP_2; thus, PIP_2 hydrolysis might induce modifications of the membrane curvature in the proximity of the TRP channel leading to its mechanical activation [128]. In other cases, the indirect activation of TRP channels might be realized through the binding of specific ligands, such as DAG, PIP_2 [131], reactive oxygen species (ROS) [134], or serotonin [155].

However, it cannot be completely excluded that TRP channels are primary mechanosensors, such as the *Drosophila* NompC channels. NompC channels are mechano-gated channels that rely on a force-from-tether model, in which the ankyrin repeats of the N-terminal form a tether linking the channel to the microtubules, usually called membrane-microtubule-connector (MMC) [102]. The force-from-tether model is further confirmed by observations that microtubules alterations result in impaired NompC functioning [102,156]. The *Drosophila* NompC channels are an example of single-step direct mechanical gating [130].

Table 1. List of mechanosensitive ion channels expressed in neurons.

Mechanosensitive Channels			
Channel	**Role**	**Expression Pattern**	**Gating Mechanism**
DEG/ENaC/ASiC			
C. elegans MEC-4/MEC-10	Gentle touch, nociception, proprioception ultrasound response [19,21–23]	Axons of touch receptors neurons [18–20]	Pore forming subunits in MeT complexs [18–20] Proposed force-from-tether model [42–44]
Mammalian ASIC	Nociception, regulation of blood pressure, regulation of gastrointestinal function [34]	Dorsal root ganglia [35,36], visceral mechanoreceptors [34,157], aortic baroreceptors neurons [33], sensory neurons of the skin [28,29]	Still debated, proposed force-from-lipid and force-from-tether models [38]
Drosophila pickpocket, ripped pocket, and balboa	*Drosophila* mechanmechannociception	Class IV multidendritic (md) [13,26,27]	Not known
K2P			
Mammalian TREK-1/2, and TRAAK	Regulation of the threshold for mechanical responses	Dorsal root ganglia	Force-from-lipid gating stretch-activated currents in heterologous expression elicited by negative-pressure
Drosophila ORK-1	Regulation of sleep and cardiac rhythm [64–66]	Heart [64]	Not known
Piezo			
Mammalian Piezo-1/2	Mammalian noxious mechanosensation	Merkel cells, hair follicles and hair cells of the auditory system	Force-from-lipid [69,84,158] is the principal mechanism for Piezo-1 but not for Piezo-2 [85]
Drosophila Piezo	*Drosophila* mechanonociception	Neuronal and non-neuronal cells	Stretch-activated currents elicited by negative pressure application [75]
C. elegans PEZO-1	Severe defects in oocyte and sperm transit [84]	Male tail sensory neurons, pharyngeal neurons, intestine and vulva [76]	Not known
Anoctamin superfamily			
Mammalian TMC-1/2	Human and mice hearing	Stereocilia of inner ear hair cells	Pore forming subunits in MeT complexes in inner ear hair cells.
Drosophila TMC-1/2	*Drosophila* propriorception and locomotion	class I and class II dendritic arborization neurons and bipolar dendrites neurons	Not known
Danio rerio TMC-1 and TMC-2	Water motion detection and hearing [95]	Stereocilia of the neuromast [95]	Pore forming subunits of MeT complexes [8]
C. elegans TMC-1 and TMC-2	Vulval muscle excitability, mechanosensation salt sensation [9,96,159]	Mechanosensory neurons [9] vulval muscles [159] ASH neurons [96]	Pore forming subunits in MeT complexes [9]

Table 2. List of mechanosensitive TRP channels expressed in neurons.

Channel	Role	Expression Pattern	Gating Mechanism
TRP Channels			
TRPN			
Drosophila NoMPC	Auditory transduction	Auditory organs and Mechanosensory bristles [160]	Activation through intracellular theters [102,115,161–163]
C. elegans TRP-4	Proprioreception [121,122]	Mechanosensory neurons [121,122]	Direct activation by force [122]
Danio rerio TRPN-1	Hearing [164]	Auditory cells [164]	Not known
TRPV			
Mammalian TRPV-1,2,4	Mechanosensation in osmosensory neurons	Myenteric neurons Dorsal root ganglia osmosensory neurons C-fibers [135,137,165–174]	Debated: stretch sensitive sensitive [135,137,138,169,170] or insensitive [131,153]
C. elegans OSM-9 and OCR-1/4	Nose-touch osmosensation [20,175,176]	Mechanosesory neurons	Indirect activation [155,177]
Drosophila iav and *nan*	Gravity and sound sensation [178–180]	Johnston'S organ [178–180]	Not known
TRPC			
Mammalian TRPC-1, TRPC-3, and TRPC-5	Ligth touch and sound responses. Blood pressure regulation [113,114,117,119,120]	Dorsal root ganglia, cochlear cells, light touch cutaneous afferents and aortic baroreceptors neurons [113,114,139,140]	Debated: stretch sensitive sensitive [139–145] or insensitive [131,152]
C. elegans TRP-1/2	Propiorception [123]	SMDD neurons [123]	Not known
TRPM			
Mammalian TRPM-4/7/8	Cell adhesion and migration shear stress detection [147,181–184]	Non neuronal cells [181–184]	Debated: stretch sensitive sensitive [127,146,147] or insensitive [131,154]
TRPP			
Drosophila BRV-1	Cold sensation Gentle touch sensation in larvae [116]	class III neurons [116]	Stretch-activation in heterologous expression [116]
C. elegans LOV-1 and PDK-2	Male mating behaviour [185,186]	Male specific sensory neurons [185,186]	Pore forming subunits of MeT complexes [185,186]
TRPA			
Mammalian TRPA	Candidates for auditory transduction [124]	Auditory cells Dorsal root ganglia [124]	Debated: stretch sensitive sensitive [124,150] or insensitive [131]
C. elegans TRPA	Nose touch [118]	OLQ and IL1 mechanosensory neurons [118]	Stretch-gated [118]
Drosophila TRPA	Noxious mechanical stimuli geotaxis [125,126,151]	Sensory neurons Johnston organ [125,126]	Activated by osmotic changes [126]

2.6. Other Mechano-Gated Proteins and Channels

All mechanotransduction mechanisms described so far are ionotropic mechanisms. Ionotropic mechanotransduction is fast and mediated by the activation of ionic channels such as the TRP, DEG/ENaC/ASIC, Piezo, or K2P channels. In addition to this fast pathway, there is another mechanotransduction pathway that works at slow time scales: the metabotropic mechanotransduction. This mechanism relies on G-protein-coupled-receptors (GPCRs), which can be activated by mechanical stimuli, such as the shear stress [187]. GPCR-mediated mechanotransduction has been observed in vascular and renal system [187]. Among the shear stress-activated GPCRs there are the angiotensin receptors of the heart tissue, the bradykinin receptors of endothelial cells, and the GPCR68 expressed in the vascular system and DRG neurons [188–190]. In a recent work, Erdogmus et al. showed that the helix 8 is essential for the mechanosensitivity of the GPCRs. Indeed, its removal is sufficient to disrupt the mechanosensitivity of the histamine receptor H_1R [191]. Despite the growing evidence of the importance of mechanosensitive GPRCs, their role in pathophysiological conditions is still very poorly explored.

3. Modeling

We here deal with the modeling of mechanosensing at multiple scales and levels of detail. In particular, we focus on three main approaches that have been pursued in the literature to explain mechanosensing functioning and mechano-electrical coupling in neurons:

- *Atomistic modeling*. Suitable for simulating single channels embedded in the membrane lipid bilayer and short timescales processes (tens of microseconds). These models have the potential to describe at the finest detail the molecular mechanisms at the basis of mechanosensing and to analyze channel kinetics in controlled environments from a mechanical and chemical point of view. The principal drawback is the high computational cost inherent in many-body dynamics.
- *Mechanosensing continuum modeling*. Appropriate to describe single channel as well as channel pools kinetics. Two approaches can be pursued in this context. The first is the continuum-version of channel-membrane systems, designed to overcome computational limitations of atomistic modeling and span different length scales. The second is the detailed modeling of channels kinetics describing states and transitions and their dependency on mechanical strains and stresses, disregarding the spatiality of the system.
- *Multiscale mechano-electrical modeling*. Fundamental to simulate the macro and microscale mechanical problem in soft biological tissues and couple the mechanical state to the electrical neuronal response. These models can take advantage of the information derived from atomistic and continuum modeling of channels' dynamic, defining suitable phenomenological and biophysical coupling laws.

3.1. Particle Dynamics Modeling of Ion Channel Mechanosensing—Lagrangian Description

A detailed atomistic molecular description, performed via a proper statistical sampling, is in principle able to capture the molecular functioning and the coupling mechanism at the channel-membrane interface. Limitations of this kind of modeling are related to size limits on the simulations, both in terms of space and time. The atomistic molecular modeling is able to describe at most isolated channels inserted in the lipid membrane and a timescale of a few tens of microseconds in the largest simulations. This level of description is able, on the other side, to disentangle the very molecular mechanism of mechanotransduction, including effects of mutations and drugs functioning, and it can provide parameters for higher-level or multiscale methods, as described in the following sections.

In this section, the very recent outcomes of molecular dynamics (MD) simulations in the investigation of lipid membrane regulation of membrane proteins are described [192], focusing on eukaryotes channels. We refer the reader to [193] for more details on molecular dynamics simulation results for the mechanosensing proteins MscS and MscL in prokaryotes.

In general, lipids of the cellular membrane may interact with membrane proteins as a whole, i.e., the membrane exerting lateral pressure on the protein transmembrane domain, or instead acting as ligands, binding in protein pockets and exercising allosteric effects.

Some atomistic simulations have been performed specifically concerning this last point, which can be viewed as related to mechanosensing, in the sense that upon concerted motion of channel protein and membrane lipids, isolated lipid chains can occupy specific binding pockets and, therefore, favor or disfavor channel opening. In particular, Kir2 and PC2 have been investigated [194–196], and specific lipid-binding sites have been identified for these channels (see Figure 5).

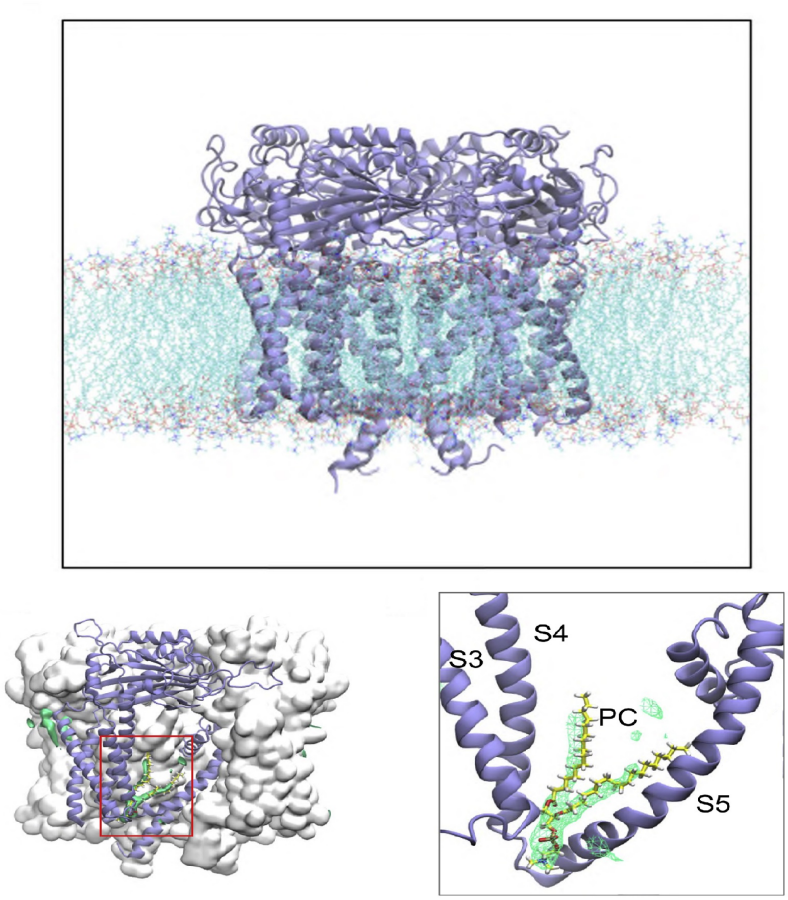

Figure 5. Identification of lipid-binding sites via molecular dynamics simulation. PC2 is an example of the identification and analysis of the role of lipids acting as a direct regulator of protein structural changes. The upper panel shows a snapshot from an molecular dynamics (MD) simulation of the PC2 channel (PDB: 5K47) embedded in the lipid bilayer. In the two bottom panels, enlargements of the protein (gray surface, with one subunit in purple) are shown, highlighting the binding pocket and the position of the lipid molecule. Adapted from [194] under the CC BY license.

However, focusing on the modeling of membrane tension and its effects on channel proteins, molecular dynamics simulations of mechanosensing channels are, overall, a quite recent success for two main reasons. First of all, the X-rays or cryo-EM structure of eukaryotes mechanosensing channels only recent became available [63,67,197–199]. Furthermore, the simulation of mechanosensing mechanism requires more than a standard MD simulation to model the effect of applied membrane tension, with simulation sizes that only recently become doable. For this reason, while several standard molecular dynamics simulations are available, characterizing various ion channels which are, among other properties, also mechanosensitive, very few studies are focused on the simulation of the

effects of membrane tension on the gating mechanism or on the role of isolated lipids in controlling the gating.

In particular, the TREK-2 channel, from the K2P family, has been recently investigated in depth [200–203] via a combination of experimental and modeling tools, and in particular via extended molecular dynamics simulations. The used MD protocol has been borrowed from previous studies on prokaryotic mechanosensitive channels to simulate the lateral tension [204]. The increasing symmetric membrane tension is simulated by increasing the lateral dimensions of the lipid bilayer. For various lateral pressure values, down to -50 bar (that is, at increasing tensions), all-atom MD simulations were performed on the TREK-2 channel in down (closed) conformation, embedded in a 1,2-palmitoyl-oleoyl-sn-glycero-3-phosphocholine (POPC) bilayer. In addition, to simulate asymmetric stresses, applied only to a single leaflet of the membrane, a slightly different protocol has been used [202], keeping fixed the lateral size of the membrane and selectively removing lipids from either inner or outer leaflets. This protocol simulates the effects of membrane curvature or of the insertion of noncylindrical lipids in the membrane. Many interesting outcomes result from this investigation [200–202]. The TREK-2 channel, subjected to increasing membrane tension, in particular to a symmetric stretch of the bilayer, undergoes a large conformational change, from the so-called 'down' conformation to the 'up' conformation, with an overall expansion of the protein section. It is worth noting that the change in the cross-sectional area of the channel is limited to the inner leaflet, while the selectivity filter region is almost unchanged upon tension. Notably, the selectivity filter is the putative location of gating in TREK-2 and TRAAK channels. Indeed, when the asymmetric stretch is applied, the increasing tension within the inner leaflet is able to induce the down-up conformational transition, similarly to the symmetric protocol, while tension applied to the outer face does not induce conformational rearrangements [202]. The relatively low values of pressure inducing the down-up conformational change are consistent with the fact that K2P channels are much more sensitive than MscL to pressure variations. Another interesting result provided by all-atom simulations is the lateral, non-homogeneous profile of the pressure, which can be characterized as a function of the depth into the membrane and of the applied tension. A comparison with a lipid bilayer producing a different pressure profile demonstrated its key role, with respect to other putative ingredients as bilayer thickness and hydrophobic mismatch, at least for the considered channel. The same MD protocol used for TREK-2, applied to the homologous but non-mechanosensitive K2P channel TWIK-1, could not obtain conformational changes, assessing the specificity of the TREK-2 channel and the quality of the atomistic modeling [200] (Figure 6). The connection between conformational states (up or down) due to applied tension and the conductive state of the channel deserves more attention [203] because the transmembrane domain is intrinsically mechanosensitive, but it is also allosterically coupled to the gating mechanisms. A striking difference between MscL and TREK-2, concerning the channel pore behavior upon membrane tension, is that the protein expansion drives the direct pore opening in MscL, while the mechanism related to the channel conductivity is more complex in TREK-2 and it retains the K^+ selectivity [201]. Indeed, the TREK-2 selectivity filter is partially affected by membrane stretch [200] because ion occupancy changes depending on applied tension, while the ionic selectivity, interestingly, is not altered by membrane stretch [201]. Overall, the MD results for TREK-2 confirm that the model force-from-lipid can successfully explain the TREK-2 behavior, that the direct lipid occlusion has a non-prevalent role in the gating mechanism, that the ionic selectivity is retained at the selectivity filter, and that the asymmetric sensitivity of TREK-2 helps in maintaining the filter structure [200–202]. Further investigations have been devoted to the relationship between conformational and conductive states of the channel by simulating TREK-2 up and down states with physiological membrane potential, together with applied membrane tension [203]. Apart from gaining even more details of the gating mechanisms, those last MD simulations could identify the down conformation as a state most probably non-

conductive, the up conformation as mostly conductive, and verify that membrane tension increases conductivity by favoring the up conformation.

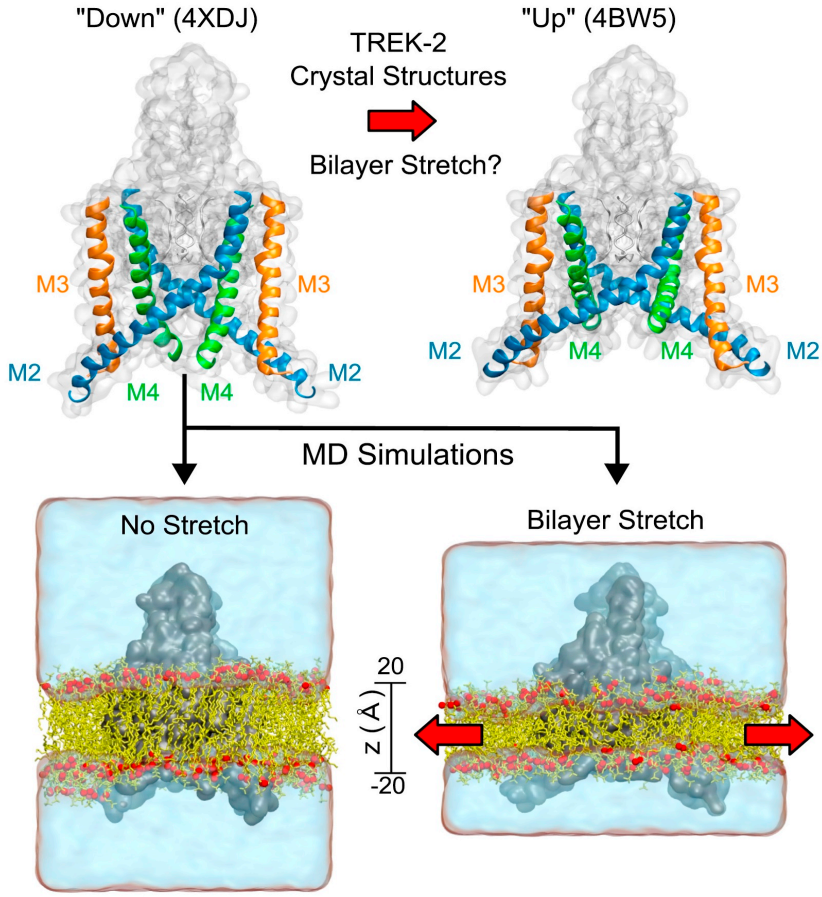

Figure 6. Membrane tension applied to the TREK-2 channel via molecular dynamics simulations. The transmembrane domain modifications induced by lateral membrane tension are shown. When the membrane is not strained, the channel is mostly in the down conformation. When tension is applied to the membrane, the channel moves towards the up conformation. The selectivity filter region, outside of the membrane, is not structurally altered by the applied tension. Adapted from [200] under the CC BY license.

The TRAAK channel, pertaining to the same K2P family, has also been modeled and studied [205] via molecular dynamics and Brownian dynamics [206]. The steric occlusion of the channel produced by lipids has been in this channel related to the loss of conduction in the closed conformation. Therefore, the direct lipid occlusion can also play a role in the complex regulation of channel proteins by the lipid membrane.

As said, the membrane-channel protein system is a typical case of multiscale systems, for which proper multiscale approaches should be used. The multiscale description may be serial, in the sense that results from a certain level of description can be used in a sequential protocol as input data for a different level of description. An example regarding the discrete description is given by the combination of coarse-grained molecular dynamics (CG-MD) and all-atom molecular dynamics. CG-MD simulations may efficiently explore membrane protein/lipid interactions, producing starting configurations to be converted to an atomistic resolution to refine and characterize the coupling [207]. The mechanosensitive ASIC channel has been used as a test case to verify the quality of the protein–lipid interface description at the coarse and atomistic level [207].

The combined CG-MD and all-atom MD approach has also been used in a recent case study, similar to TREK-2, provided by Piezo1 [208]. Its activation mechanism, related to the

transition from closed to open conformation, is due to structural rearrangements related to cell membrane tension. Piezo1 has been investigated within a two-step, multiscale protocol. An initial coarse-grained molecular dynamics (CG-MD), using the Martini force field, has been performed to obtain the initial conformation, with a complex asymmetric membrane conformation. Piezo1 has an initial stable conformation characterized by a curved shape, with indentated membrane at rest. Once stabilized, the system has been converted to an all-atom description. The membrane stretching protocol is similar to the one used for TREK-2 [200]. Upon membrane stretching, both membrane and Piezo1 flatten, and Piezo1 expands, remaining embedded in the lipid bilayer. The extracellular domain becomes more exposed upon Piezo1 flattening, and the water-filled region inside the pore increases. Therefore, the applied membrane tension drives the channel opening. Due to the structural similarities between Piezo1 and Piezo2, it is hypothesized that the same mechanism holds for Piezo2 [208] (Figure 7).

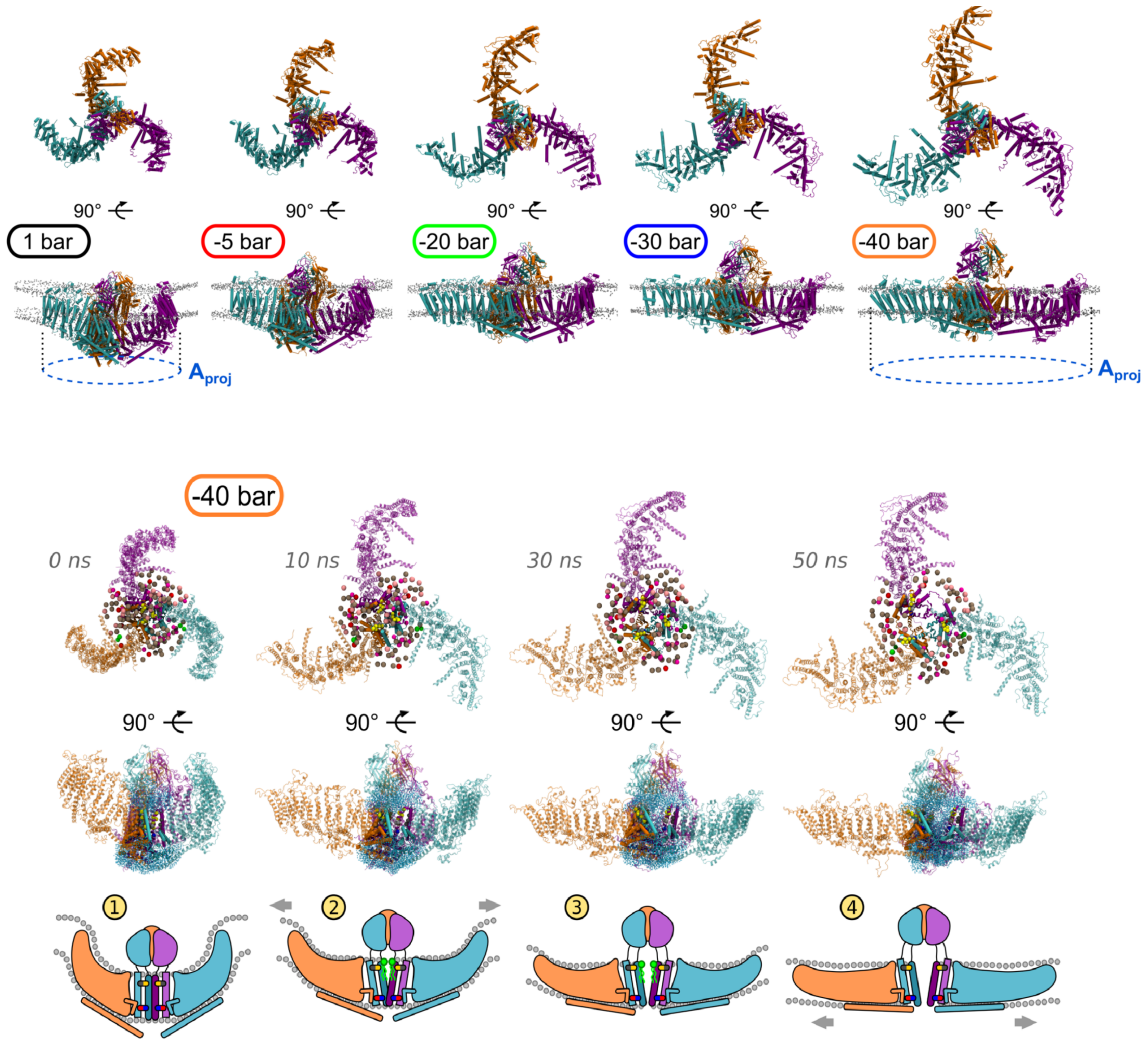

Figure 7. Membrane tension applied to Piezo1 channel via molecular dynamics simulations. In the upper panel, top and lateral views of Piezo1 channel flattening upon increasing membrane tension, up to −40 bar. In the lower panel, a sequence of snapshots from MD simulation at −40 bar, extracellular top view and lateral view, and cartoon representation explaining the Piezo1 activation mechanism coupled to membrane tension. Grey arrows indicate membrane tension and Piezo1 blade expansion. Adapted from [208], under CC–BY–NC–ND 4.0 International license.

The molecular dynamics is, therefore, a powerful tool to describe and understand at the molecular level the functioning of mechanosensing channels, and its desirable

application to other families of MS proteins would provide much more information that could also be included in multiscale continuum descriptions.

3.2. Continuum Modeling of Ion Channel Mechanosensing—Eulerian Description

The multiscale description necessary to study mechanotransduction can be afforded via continuum models that can mimic various mechanisms contributing to channel activation. The continuum models have been so far only applied, to the author's best knowledge, to scL channels, systems in which the pressure-driven gating mechanism is directly related to the channel opening, therefore less complex than in the case of TREK-2 or Piezo1 described above in terms of all-atom models.

A possible continuum mechanics-based simulation method, called Molecular Dynamics-decorated Finite Element Method (MDeFEM) [209] is based on the description of the membrane as an elastic/viscoelastic medium, whose mechanical properties are obtained from molecular dynamics, as well as the coupling parameters with the embedded channel protein. The channel proteins are modeled as combinations of elastic continuum structures, whose motion (collective behavior) is described by the lowest modes obtained from the principal component analysis. The method can, in principle, couple different length scales and manage corresponding loadings, and it has been successfully applied to MscL [209]. A similar method, with some differences in the details of the system description, has been used more recently to study MscL [210], with a special focus on the combined effect of membrane bending and hydrophobic mismatch. The representative volume element (RVE) model of MscL is able to describe the channel pore corresponding to various functional states (in detergent, resting, and open [210]). The hydrophobic pairwise interaction between protein and bilayer is also included. The study identified the most favorable condition for MscL gating in the local bending together with zero hydrophobic mismatch and found that inward bending (negative bending) is more effective for MscL opening compared to outward (positive) bending.

An important modeling step is the proper evaluation of microscopic stresses [211,212], that connect the membrane continuum [211] to the protein described, via statistical mechanics, at the atomistic level. In some mathematical definitions of microscopic stress, some ambiguity may emerge, in particular when applied to complex materials, including protein–lipid assemblies. A detailed mathematical definition of microscopic stress tension has been recently developed, based on an accurate decomposition of forces even for many-body potentials [211,212]. The most detailed description of continuum microscopic stresses obtained from discrete systems mechanics is based on the Irving–Kirkwood (IK) stress definition for two-body interactions, extended to include the central force decomposition (CFD) for treating the many-body potentials and satisfying the mechanical equilibrium laws. The method, applied to a lipid bilayer, successfully incorporates the details of membrane layered and torquing stress. Therefore, it is important to use a reliable definition to evaluate microscopic stress to derive microscopic properties from MD simulations to be implemented in continuum models.

A generalized model for the activation of MeT channels in *C. elegans* [213] is based on the main idea of coupling, in a suited manner, MeT channels to the viscoelastic medium subject to external stimuli, and including in the description the dynamics of MeT gating, modeled in a mean-field theory framework. The coupling to the viscoelastic medium is modeled with each MeT channel linked to a mechanical anchor via an elastic filament. Both the filament and the anchor are embedded in the viscoelastic extracellular matrix. External strain induces a displacement between the channels and their anchors. Two other forces act on the filament/anchor systems, the elastic force due to the elongation of the elastic filament and the friction forces between the extracellular matrix and the filament/anchor system. Both forces are suitably represented with springs. Figure 8 represents a sketch of the proposed MeT channels gating mechanism.

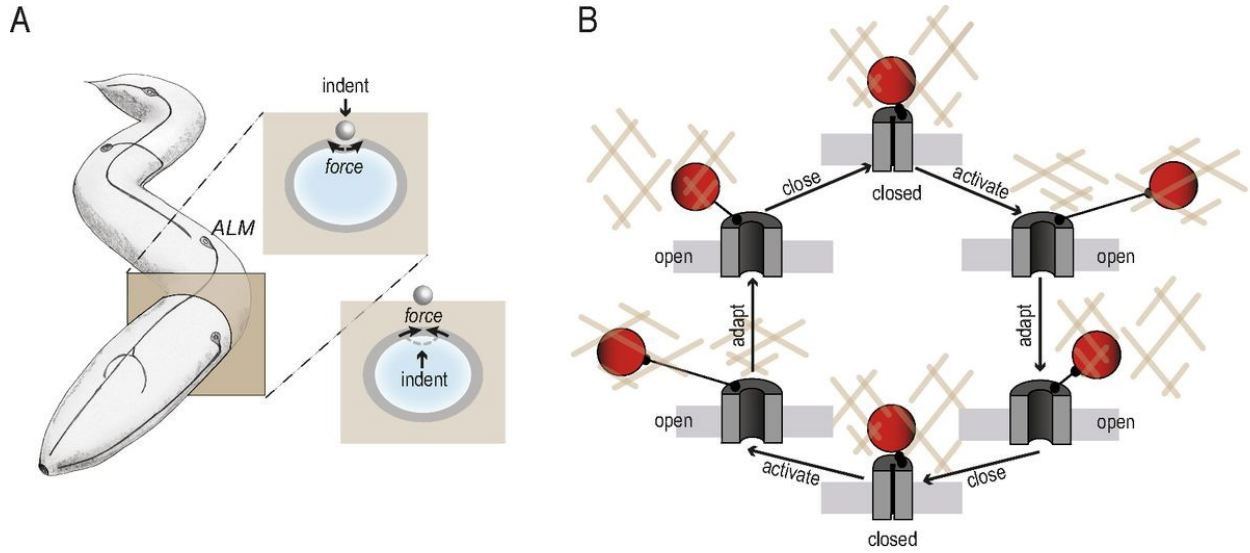

Figure 8. Gating mechanism of MeT channels in *C. elegans* touch receptor neurons (TRNs). (**A**) Schematic representation of the forces acting on TRNs in consequence of cuticle indentation. (**B**) Schematic representation of a possible gating model of MeT channels. An elastic filament links the channel to an anchor that moves in the extracellular matrix [213]. In clockwise order from top to bottom: a deformation applied to the extracellular matrix causes a lateral shift between the anchor and the matrix and induces a stretch of the filament that activates the channel. Viscoelastic forces allow the filament to return into its relaxed state, inducing the channel adaption and closure. When the external deformation is released, a second lateral shift of the anchor with respect to the extracellular matrix occurs, resulting in the channel opening. Finally, the initial configuration is restored by viscoelastic forces. Figure adapted from [213] under the exclusive License to Publish.

Concerning the gating dynamics, the opening/closing of a single MeT channel is driven by two factors: the filament elongation, inducing the channel opening, and the statistical probability of the channel being in a conductive state. The gating dynamic is described by three states (open, closed, and subconducting) and by their transition rates. A realistic model should describe the different effects of membrane stretch at different positions in the viscoelastic medium. To overcome the complexity of a point-like description to describe the response of many MeT channels in different spatial locations, the membrane tension and its effect on elastic filaments are described via a mean-field method. Overall, the population of MeT channels is collapsed in a unique, effective MeT channel, whose gating dynamics overall takes into account the statistical response of a region of space with embedded MeT channels. The obtained effective channel, based on available experimental data, describes the dynamics of 15–30 actual channels, in good agreement with activated channels as estimated from experimental data. The inclusion of higher-order mechanical effects in the model shall require more detailed experimental data. Notably, biophysical modeling of mechano-activated channels can take inspiration from other detailed models built for different transduction mechanisms, e.g., [214,215].

3.3. Multiscale Mechano-Electrical Modeling

In this section, we discuss modeling studies dealing with the multiscale coupling of cells or tissue mechanics to the electrophysiological response of neurons. Those applications range from descriptions of mechano-electrical coupling at the single neuron level in simplified loading conditions to more realistic modeling investigations, including complex mechanical problems at the tissue level.

In the context of simplified loading mechanical conditions, Jérusalem et al. [216] adopted a multiscale mathematical model to investigate the effect of spinal cord injury and mechanical damage on myelinated axons' electrical response. In particular, they formulated a mechanical model of the myelinated axon-extracellular matrix system, comprising a Maxwell material for the axon in parallel to a viscoelastic material for the surroundings. They also included irreversible plastic damage in the model and assumed a small strain

regime and quasi-static conditions. The microscopic axial strain is opportunely split into two contributions from Nodes of Ranvier (NRs) and Internodal Regions (IRs). Axon incompressibility is further used to couple the axial strain to cell membrane strain and diameter deformations of both surface membrane and myelin layers. Finally, axon electrical response is modeled via Hodgkin–Huxley and Cable theories, where electrical parameters of myelin layers and cell membranes depend on the corresponding mechanical state by means of the strain. Among the electrical parameters affected by the strain, we can find membrane capacitance, axial and membrane resistance, ion conductances, Nernst potentials, and steady-state activation/inactivation functions of ion channels' dynamics. The model is calibrated on tensile tests on guinea pig spinal cord nerves, performed at variable axial strain rates and different maximum applied strains. Model results show action potentials (AP) impairment after the removal of damaging loads consistent with experiments.

Another interesting contribution in the same direction comes from Tian et al. [217], who analyze alterations in action potential (AP) propagation in neurons subjected to stretching and plastic deformations. Compared to Jérusalem et al., their model is based on a slightly modified mechanical description, relying on power-law responses of neuronal deformations and a similar electrical compartment and mechano-electrical coupling. Simulations results are consistent with experimental observations and show AP suppression, increased spiking frequency, and altered conduction velocity at increasing axial strains.

Additional efforts in coupling mechanics to electrophysiology in nerves focused instead on the analysis of pressure waves traveling along the axon as induced by action potential propagation (Engelbrecht et al. [218]). In this study, it is considered both the electromechanical and the mechano-electrical coupling. In particular, pressure, longitudinal and transversal mechanical waves along the cell membrane, modeled as a two-dimensional elastic cylinder, are assumed to be triggered by forces induced by local excitations of the nerve, and the longitudinal displacement due to mechanical waves affects back electrical activation through proper forcing terms. Longitudinal and transversal waves are described based on the Heimburg and Jackson model for biomembranes and theory of rods, respectively. Electrical activation is reproduced with a FitzHugh–Nagumo model, generalized to include mechanical activation.

An interesting application of multiscale modeling, coupling mechanics and neuronal dynamics, concerns the mechanotransduction in skin. In this direction, Sripati et al. [219] formulated a model to reproduce the stimulus-response coupling in cutaneous slowly adapting 1 (SA1) and rapidly adapting afferent fibers, innervating Merkel and Meissner corpuscles, respectively. The model includes a continuum mechanical description of skin, allowing for predictions of strain profiles in response to applied loads. The skin is modeled as a linear elastic, homogeneous, and isotropic medium, and its mechanical state is described based on the Timoshenko and Goodier stress model for a point load, on a decomposition of the stress on a basis of such unit point-load responses, and on the Hooke's constitutive law. The skin's mechanical state is phenomenologically coupled to the afferent fibers' discharge rate by fitting models' parameters to reproduce experimental data recorded on monkeys. Interestingly, a combination of mechanical variables satisfying specific rotational invariance properties is included in the coupling term, among which the maximum compressive and tensile strains (and stresses), the vertical strain (and stress), the maximum horizontal strain (and stress), the maximum deformative strain (and stress), the sum and product of the strain eigenvalues, and the strain energy density. In regards to mechanotransduction in SA1 fibers, a further contribution by Lesniak et al. [220] introduced an interesting model coupling the skin mechanics to an integrate-and-fire electrical compartment to reproduce neuronal discharges. In this study, the authors built an FEM linear elastic model of fingertip skin reproducing skin's microstructure and multilayer composition. A strain energy density for nearly incompressible material, defined by means of the octahedral shear stress, is used to couple the mechanical state of the fingertip to the electrical response of the afferent fibers, whose neuronal dynamics are reproduced with a classic leaky integrate-and-fire (LIF) description. The coupling term is represented by

a specific receptor current whose activation is shaped via sigmoidal function, dependent on the strain energy density. In this case, also, model parameters are fitted to reproduce experimental data recorded on monkeys. A similar and more novel contribution dealing with multiscale modeling of Merkel cell-SA1 fiber complex comes from Gerling et al. [221]. In this study, the authors formulated a model based on three components: a skin FEM model, a current-generator function, and a leaky integrate-and-fire electrical model.

The skin model is based on a multilayer description and on a quasi-linear viscoelastic material, with parameters fitted on mouse skin data, and permits to compute compressive stresses within the skin in response to ramp-and-hold displacement stimuli. The generator function basically couples the stress' dynamic to a stimulating current composed of fast-inactivating, slowly-inactivating, and ultra-slowly-inactivating components. The coupling is performed through a convolution of the time derivative of the stress profile with different exponential functions describing the output for each current component in response to a step-stress stimulation. The total induced current is taken as input in an LIF model of neuronal response. Figure 9 shows the general modeling concept.

Detailed multiscale models were also developed for mechanotransduction in Pacinian corpuscles (PCs). In a specific application, Quindlen et al. [222] developed a comprehensive description of the PC based on finite-element models of the PC's outer and inner regions, and a detailed model of a neurite included in the PC. In this study, the mechanical description of the PC's outer shell accounts for both lamellar spherical shells and an interlamellar fluid component. In addition, the inner core is modeled as a linear elastic isotropic sphere, including a cylindrical neurite with a spherical ending, enriched with smaller cylinders to reproduce the neurite's filopodia. The outer shell model is stimulated by periodic pressure profiles applied at the outer surface at different frequencies, predicting the displacement of each spherical shell. The displacement of the inner shell is then used as a boundary condition for the inner core mechanical model, which permits the computation of the mechanical state of the neurite. Finally, the mechanical state of the neurite is used to modulate a stretch-gated ion current in a biophysical Hodgkin–Huxley (HH) neurite implemented in the NEURON environment. This sub-model includes classic HH potassium and sodium currents and point current sources to simulate stretch-activated channels, whose maximum current value is modulated by the neurite's strain through a sigmoidal activation function.

Another interesting multiscale model of mechanotransduction concerns the touch sensing in *C. elegans*. In this particular scenario, Sanzeni et al. [223] presented a detailed model coupling the macroscopic nonlinear mechanics of the nematode body to the activation of MeT channels in touch receptor neurons. The authors develop a model accounting for the mechanical deformation of the worm in response to the application of glass probes or microbeads and a generalized model of the activation of MeT channels, based on the work by Eastwood et al. [213]. In particular, the worm is modeled as a thin elastic cylindrical shell in a regime of large deformations (Figure 10). At the microscale level, MeT channels' activation is coupled to the displacement field computed by the mechanical model by assuming that each channel is connected to an elastic filament giving rise to elastic and friction forces. The computation of the filaments extension and the resulting elastic forces along the membrane tangential component is further used to modulate the change in free energy between MeT ion channels' states and compute the activation of ion channels' populations and the induced mechanosensitive current.

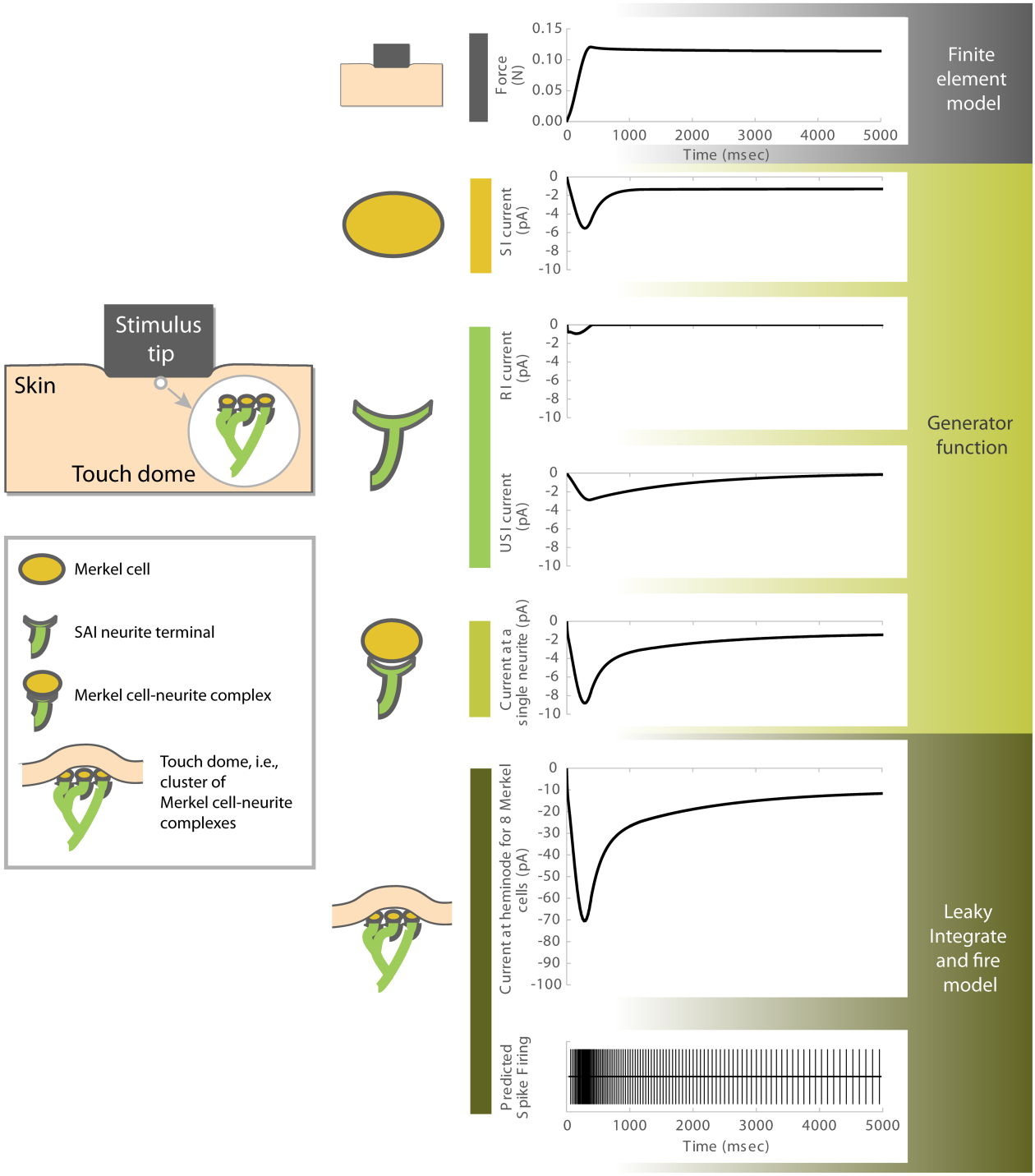

Figure 9. Schematic representation of multiscale model of Merkel cell-neurite complexes. The top panel on the right shows the stimulus applied to the skin. SI and USI represent the slowly–activating current arising from the Merkel–cell and the ultra–slowly–inactivating from the neurite terminal. The generator function includes the three currents and the compressive stress and uses as input the compressive stress calculated from the stimulus force (top panel) through a finite–element model. The simulated currents for a single Merkel–cell are summed to obtain a heminode constituted by eight Merkel–cell neurite complexes. Reproduced from [221] under the CC BY license.

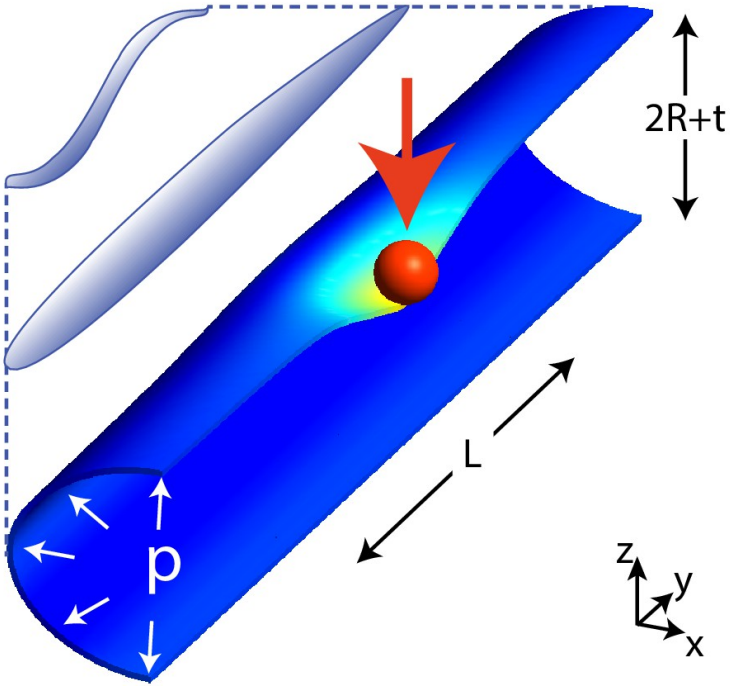

Figure 10. Schematic representation of *C. elegans* body and mechanics. A cylindrical shell 1 mm long and with a radius of about 25 µm is used. Such a shell is indented by the application of a spherical bead. The symbol t denotes the thickness of the shell. Reproduced from [223] under the CC BY license.

4. Discussion and Conclusions

In this contribution, we reviewed the main ion channels expressed in neurons directly involved in mechanosensation and in transducing mechanical signals from the environment in specific electrical outputs and provided a comprehensive description of available theoretical frameworks successfully applied to the investigation of mechanosensing at different scales.

The identified MS ion channels superfamilies include DEG/ENaC/ASIC, K2P, PIEZO, Anoctamin, and TRP channels. These channels are expressed both in specialized cells and in sensory neurons and share similar properties in the underlying mechanisms of channels' gating. Those specific properties permit mechanical sensing by means of stretch and stress thanks to interactions between ion channels, cell membrane, cytoskeleton, and ECM. The gating of all those channels is regulated by complex mechanisms, including the two main contributions given by lipid- and tether-transmitted forces, and it is reasonable to assume that those features are opportunely combined to achieve optimal mechanical sensitivity.

In the last years, several efforts have been devoted to the investigation of MS channels' gating and to the development of accurate models able to describe channels' activation in response to mechanical stimulation. Those models were developed on different levels of detail, including the molecular and the cell/tissue scales. Our analysis on atomistic and molecular dynamics approaches to the investigation of MS channels showed that modeling could enlighten key features in MS channel gating, and, up to now, such approaches were able to highlight important mechanisms involved in the lipid-force-driven gating of specific MS channels types. MD derived properties can also be used to develop the continuum description of mechanotransduction, based on viscoelastic modeling of the membrane coupled to mechanic models of ion channels. It is worth noting that the increasing complexity of gating mechanisms, from MscL to mammalian Piezo1, that can be described at the atomistic level, will contribute to developing more refined continuum models, with the advantage of simulating larger systems and a wider range of mechanical stimulations. Such descriptions can be eventually used to obtain macroscopic parameters to be included in coarse electrophysiological models of whole-cell mechano-gated ion currents. Concerning

modeling of mechanosensation in neurons at the whole-cell scale and the tissue scale, we further showed that the microscale activation of MS channels in neurons could be coupled to the embedding tissue's biomechanics to achieve a comprehensive description of the whole mechanotransduction process. However, most of these multiscale descriptions are based on simplistic models of neuronal dynamics, mechano-electrical coupling, and tissue biomechanics and still need to be refined and generalized to achieve a higher degree of realism and descriptive/predictive power. In particular, other statistical mechanics tools, multiphysics couplings, and more detailed biomechanical and electrophysiological models can be introduced, as performed in modeling studies on different biological systems [224–234]. In addition, to achieve a better description of mechanotransduction, further studies focused on the electrophysiological dissection of mechano-gated current should be performed. In principle, this information can be merged with atomistic single-channels simulations and is crucial to built reliable biophysical models of neuronal dynamics at the whole-cell scale. Indeed, our research identified only a small amount of papers presenting those data but limited only to MS macro-currents or not reporting a full characterization of the ion currents with respect to the mechanical state. On this basis, future efforts should be devoted both to the generalization and development of atomistic, electrophysiological, and multiscale models, not only to grasp key features in neuron mechanotransduction but also to translate this knowledge to the design of bioinspired tools and devices.

Author Contributions: Conceptualization, M.N., L.C. and A.L.; methodology, M.N., L.C. and A.L.; resources, M.N., L.C. and A.L.; writing—original draft, M.N., L.C. and A.L.; preparation, M.N., L.C. and A.L.; writing—review and editing, M.N., L.C. and A.L.; visualization, M.N., L.C. and A.L.; supervision, A.L. All authors have read and agreed to the published version of the manuscript.

Funding: This research received no external funding.

Institutional Review Board Statement: Not Applicable.

Informed Consent Statement: Not Applicable.

Data Availability Statement: Not Applicable.

Acknowledgments: M.N., L.C., and A.L. acknowledge the support of Gruppo Nazionale per la Fisica Matematica (GNFM-INdAM).

Conflicts of Interest: The authors declare no conflict of interest.

References

1. Árnadóttir, J.; Chalfie, M. Eukaryotic mechanosensitive channels. *Annu. Rev. Biophys.* **2010**, *39*, 111–137. [CrossRef] [PubMed]
2. Martinac, B.; Cox, C. Mechanosensory transduction: Focus on ion channels. In *Reference Module in Life Sciences. Edition: Comprehensive Biophysics*; Elsevier BV: Amsterdam, The Netherlands, 2017.
3. Ranade, S.S.; Syeda, R.; Patapoutian, A. Mechanically activated ion channels. *Neuron* **2015**, *87*, 1162–1179. [CrossRef] [PubMed]
4. Marcovich, I.; Holt, J.R. Evolution and Function of Tmc Genes in Mammalian Hearing. *Curr. Opin. Physiol.* **2020**, *18*, 11–19. [CrossRef]
5. Zhao, B.; Wu, Z.; Grillet, N.; Yan, L.; Xiong, W.; Harkins-Perry, S.; Müller, U. TMIE is an essential component of the mechanotransduction machinery of cochlear hair cells. *Neuron* **2014**, *84*, 954–967. [CrossRef]
6. Maeda, R.; Kindt, K.S.; Mo, W.; Morgan, C.P.; Erickson, T.; Zhao, H.; Clemens-Grisham, R.; Barr-Gillespie, P.G.; Nicolson, T. Tip-link protein protocadherin 15 interacts with transmembrane channel-like proteins TMC1 and TMC2. *Proc. Natl. Acad. Sci. USA* **2014**, *111*, 12907–12912. [CrossRef]
7. Beurg, M.; Xiong, W.; Zhao, B.; Müller, U.; Fettiplace, R. Subunit determination of the conductance of hair-cell mechanotransducer channels. *Proc. Natl. Acad. Sci. USA* **2015**, *112*, 1589–1594. [CrossRef] [PubMed]
8. Erickson, T.; Morgan, C.P.; Olt, J.; Hardy, K.; Busch-Nentwich, E.; Maeda, R.; Clemens, R.; Krey, J.F.; Nechiporuk, A.; Barr-Gillespie, P.G.; et al. Integration of Tmc1/2 into the mechanotransduction complex in zebrafish hair cells is regulated by Transmembrane O-methyltransferase (Tomt). *Elife* **2017**, *6*, e28474. [CrossRef]
9. Tang, Y.Q.; Lee, S.A.; Rahman, M.; Vanapalli, S.A.; Lu, H.; Schafer, W.R. Ankyrin Is An Intracellular Tether for TMC Mechanotransduction Channels. *Neuron* **2020**, *107*, 112–125. [CrossRef] [PubMed]
10. Ballesteros, A.; Fenollar-Ferrer, C.; Swartz, K.J. Structural relationship between the putative hair cell mechanotransduction channel TMC1 and TMEM16 proteins. *Elife* **2018**, *7*, e38433. [CrossRef] [PubMed]

11. Xiong, W.; Grillet, N.; Elledge, H.M.; Wagner, T.F.; Zhao, B.; Johnson, K.R.; Kazmierczak, P.; Müller, U. TMHS is an integral component of the mechanotransduction machinery of cochlear hair cells. *Cell* **2012**, *151*, 1283–1295. [CrossRef] [PubMed]
12. Giese, A.P.; Tang, Y.Q.; Sinha, G.P.; Bowl, M.R.; Goldring, A.C.; Parker, A.; Freeman, M.J.; Brown, S.D.; Riazuddin, S.; Fettiplace, R.; et al. CIB2 interacts with TMC1 and TMC2 and is essential for mechanotransduction in auditory hair cells. *Nat. Commun.* **2017**, *8*, 43. [CrossRef] [PubMed]
13. Mauthner, S.E.; Hwang, R.Y.; Lewis, A.H.; Xiao, Q.; Tsubouchi, A.; Wang, Y.; Honjo, K.; Skene, J.P.; Grandl, J.; Tracey, W.D., Jr. Balboa binds to pickpocket in vivo and is required for mechanical nociception in *Drosophila* larvae. *Curr. Biol.* **2014**, *24*, 2920–2925. [CrossRef]
14. Noreng, S.; Bharadwaj, A.; Posert, R.; Yoshioka, C.; Baconguis, I. Structure of the human epithelial sodium channel by cryo-electron microscopy. *Elife* **2018**, *7*, e39340. [CrossRef] [PubMed]
15. Eastwood, A.L.; Goodman, M.B. Insight into DEG/ENaC channel gating from genetics and structure. *Physiology* **2012**, *27*, 282–290. [CrossRef]
16. Jasti, J.; Furukawa, H.; Gonzales, E.B.; Gouaux, E. Structure of acid-sensing ion channel 1 at 1.9 Å resolution and low pH. *Nature* **2007**, *449*, 316–323. [CrossRef] [PubMed]
17. Zelle, K.M.; Lu, B.; Pyfrom, S.C.; Ben-Shahar, Y. The genetic architecture of degenerin/epithelial sodium channels in *Drosophila*. *G3 Genes Genomes Genet.* **2013**, *3*, 441–450.
18. Chen, Y.; Bharill, S.; Isacoff, E.Y.; Chalfie, M. Subunit composition of a DEG/ENaC mechanosensory channel of *Caenorhabditis elegans*. *Proc. Natl. Acad. Sci. USA* **2015**, *112*, 11690–11695. [CrossRef] [PubMed]
19. O'Hagan, R.; Chalfie, M.; Goodman, M.B. The MEC-4 DEG/ENaC channel of *Caenorhabditis elegans* touch receptor neurons transduces mechanical signals. *Nat. Neurosci.* **2005**, *8*, 43–50. [CrossRef] [PubMed]
20. Goodman, M.B.; Ernstrom, G.G.; Chelur, D.S.; O'Hagan, R.; Yao, C.A.; Chalfie, M. MEC-2 regulates *C. elegans* DEG/ENaC channels needed for mechanosensation. *Nature* **2002**, *415*, 1039–1042. [CrossRef]
21. Tao, L.; Porto, D.; Li, Z.; Fechner, S.; Lee, S.A.; Goodman, M.B.; Xu, X.S.; Lu, H.; Shen, K. Parallel processing of two mechanosensory modalities by a single neuron in *C. elegans*. *Dev. Cell* **2019**, *51*, 617–631. [CrossRef]
22. Chatzigeorgiou, M.; Yoo, S.; Watson, J.D.; Lee, W.H.; Spencer, W.C.; Kindt, K.S.; Hwang, S.W.; Miller, D.M., III; Treinin, M.; Driscoll, M.; et al. Specific roles for DEG/ENaC and TRP channels in touch and thermosensation in *C. elegans* nociceptors. *Nat. Neurosci.* **2010**, *13*, 861–868. [CrossRef]
23. Kubanek, J.; Shukla, P.; Das, A.; Baccus, S.A.; Goodman, M.B. Ultrasound elicits behavioral responses through mechanical effects on neurons and ion channels in a simple nervous system. *J. Neurosci.* **2018**, *38*, 3081–3091. [CrossRef] [PubMed]
24. Shi, S.; Mutchler, S.M.; Blobner, B.M.; Kashlan, O.B.; Kleyman, T.R. Pore-lining residues of MEC-4 and MEC-10 channel subunits tune the *Caenorhabditis elegans* degenerin channel's response to shear stress. *J. Biol. Chem.* **2018**, *293*, 10757–10766. [CrossRef] [PubMed]
25. Shi, S.; Luke, C.J.; Miedel, M.T.; Silverman, G.A.; Kleyman, T.R. Activation of the *Caenorhabditis elegans* degenerin channel by shear stress requires the MEC-10 subunit. *J. Biol. Chem.* **2016**, *291*, 14012–14022. [CrossRef]
26. Tsubouchi, A.; Caldwell, J.C.; Tracey, W.D. Dendritic filopodia, Ripped Pocket, NOMPC, and NMDARs contribute to the sense of touch in *Drosophila* larvae. *Curr. Biol.* **2012**, *22*, 2124–2134. [CrossRef] [PubMed]
27. Ainsley, J.A.; Pettus, J.M.; Bosenko, D.; Gerstein, C.E.; Zinkevich, N.; Anderson, M.G.; Adams, C.M.; Welsh, M.J.; Johnson, W.A. Enhanced locomotion caused by loss of the *Drosophila* DEG/ENaC protein Pickpocket1. *Curr. Biol.* **2003**, *13*, 1557–1563. [CrossRef]
28. Cabo, R.; Galvez, M.; San Jose, I.; Laurà, R.; López-Muñiz, A.; García-Suárez, O.; Cobo, T.; Insausti, R.; Vega, J. Immunohistochemical localization of acid-sensing ion channel 2 (ASIC2) in cutaneous Meissner and Pacinian corpuscles of Macaca fascicularis. *Neurosci. Lett.* **2012**, *516*, 197–201. [CrossRef]
29. Chen, C.C.; Wong, C.W. Neurosensory mechanotransduction through acid-sensing ion channels. *J. Cell. Mol. Med.* **2013**, *17*, 337–349. [CrossRef] [PubMed]
30. Price, M.P.; McIlwrath, S.L.; Xie, J.; Cheng, C.; Qiao, J.; Tarr, D.E.; Sluka, K.A.; Brennan, T.J.; Lewin, G.R.; Welsh, M.J. The DRASIC cation channel contributes to the detection of cutaneous touch and acid stimuli in mice. *Neuron* **2001**, *32*, 1071–1083. [CrossRef]
31. Montaño, J.; Calavia, M.; García-Suárez, O.; Suarez-Quintanilla, J.A.; Gálvez, A.; Pérez-Piñera, P.; Cobo, J.; Vega, J. The expression of ENa+ C and ASIC2 proteins in Pacinian corpuscles is differently regulated by TrkB and its ligands BDNF and NT-4. *Neurosci. Lett.* **2009**, *463*, 114–118. [CrossRef]
32. Rahman, F.; Harada, F.; Saito, I.; Suzuki, A.; Kawano, Y.; Izumi, K.; Nozawa-Inoue, K.; Maeda, T. Detection of acid-sensing ion channel 3 (ASIC3) in periodontal Ruffini endings of mouse incisors. *Neurosci. Lett.* **2011**, *488*, 173–177. [CrossRef] [PubMed]
33. Lu, Y.; Ma, X.; Sabharwal, R.; Snitsarev, V.; Morgan, D.; Rahmouni, K.; Drummond, H.A.; Whiteis, C.A.; Costa, V.; Price, M.; et al. The ion channel ASIC2 is required for baroreceptor and autonomic control of the circulation. *Neuron* **2009**, *64*, 885–897. [CrossRef]
34. Page, A.J.; Brierley, S.M.; Martin, C.M.; Martinez-Salgado, C.; Wemmie, J.A.; Brennan, T.J.; Symonds, E.; Omari, T.; Lewin, G.R.; Welsh, M.J.; et al. The ion channel ASIC1 contributes to visceral but not cutaneous mechanoreceptor function. *Gastroenterology* **2004**, *127*, 1739–1747. [CrossRef]
35. Papalampropoulou-Tsiridou, M.; Labrecque, S.; Godin, A.G.; De Koninck, Y.; Wang, F. Differential Expression of Acid—Sensing Ion Channels in Mouse Primary Afferents in Native and Injured Conditions. *Front. Cell. Neurosci.* **2020**, *14*, 103 [CrossRef] [PubMed]

36. Lin, S.H.; Cheng, Y.R.; Banks, R.W.; Min, M.Y.; Bewick, G.S.; Chen, C.C. Evidence for the involvement of ASIC3 in sensory mechanotransduction in proprioceptors. *Nat. Commun.* **2016**, *7*, 11460. [CrossRef] [PubMed]
37. Garcísa-Añoveros, J.; Samad, T.A.; Žuvela-Jelaska, L.; Woolf, C.J.; Corey, D.P. Transport and localization of the DEG/ENaC ion channel BNaC1α to peripheral mechanosensory terminals of dorsal root ganglia neurons. *J. Neurosci.* **2001**, *21*, 2678–2686. [CrossRef]
38. Cheng, Y.R.; Jiang, B.Y.; Chen, C.C. Acid-sensing ion channels: Dual function proteins for chemo-sensing and mechano-sensing. *J. Biomed. Sci.* **2018**, *25*, 46. [CrossRef] [PubMed]
39. Jones, R.C.W.; Xu, L.; Gebhart, G. The mechanosensitivity of mouse colon afferent fibers and their sensitization by inflammatory mediators require transient receptor potential vanilloid 1 and acid-sensing ion channel 3. *J. Neurosci.* **2005**, *25*, 10981–10989. [CrossRef] [PubMed]
40. Bielefeldt, K.; Davis, B.M. Differential effects of ASIC3 and TRPV1 deletion on gastroesophageal sensation in mice. *Am. J. Physiol.-Gastrointest. Liver Physiol.* **2008**, *294*, G130–G138. [CrossRef] [PubMed]
41. Barth, D.; Fronius, M. Shear force modulates the activity of acid-sensing ion channels at low pH or in the presence of non-proton ligands. *Sci. Rep.* **2019**, *9*, 6781. [CrossRef] [PubMed]
42. Chalfie, M. Neurosensory mechanotransduction. *Nat. Rev. Mol. Cell Biol.* **2009**, *10*, 44–52. [CrossRef] [PubMed]
43. Emtage, L.; Gu, G.; Hartwieg, E.; Chalfie, M. Extracellular proteins organize the mechanosensory channel complex in *C. elegans* touch receptor neurons. *Neuron* **2004**, *44*, 795–807. [CrossRef] [PubMed]
44. Bounoutas, A.; O'Hagan, R.; Chalfie, M. The multipurpose 15-protofilament microtubules in *C. elegans* have specific roles in mechanosensation. *Curr. Biol.* **2009**, *19*, 1362–1367. [CrossRef]
45. Cueva, J.G.; Mulholland, A.; Goodman, M.B. Nanoscale organization of the MEC-4 DEG/ENaC sensory mechanotransduction channel in *Caenorhabditis elegans* touch receptor neurons. *J. Neurosci.* **2007**, *27*, 14089–14098. [CrossRef] [PubMed]
46. Chelur, D.S.; Ernstrom, G.G.; Goodman, M.B.; Yao, C.A.; Chen, L.; O'Hagan, R.; Chalfie, M. The mechanosensory protein MEC-6 is a subunit of the *C. elegans* touch-cell degenerin channel. *Nature* **2002**, *420*, 669–673. [CrossRef]
47. Zhang, S.; Arnadottir, J.; Keller, C.; Caldwell, G.A.; Yao, C.A.; Chalfie, M. MEC-2 is recruited to the putative mechanosensory complex in *C. elegans* touch receptor neurons through its stomatin-like domain. *Curr. Biol.* **2004**, *14*, 1888–1896. [CrossRef] [PubMed]
48. Brown, A.L.; Liao, Z.; Goodman, M.B. MEC-2 and MEC-6 in the *Caenorhabditis elegans* sensory mechanotransduction complex: Auxiliary subunits that enable channel activity. *J. Gen. Physiol.* **2008**, *131*, 605–616. [CrossRef]
49. Omerbašić, D.; Schuhmacher, L.N.; Sierra, Y.A.B.; Smith, E.S.J.; Lewin, G.R. ASICs and mammalian mechanoreceptor function. *Neuropharmacology* **2015**, *94*, 80–86. [CrossRef]
50. Wetzel, C.; Hu, J.; Riethmacher, D.; Benckendorff, A.; Harder, L.; Eilers, A.; Moshourab, R.; Kozlenkov, A.; Labuz, D.; Caspani, O.; et al. A stomatin-domain protein essential for touch sensation in the mouse. *Nature* **2007**, *445*, 206–209. [CrossRef] [PubMed]
51. Brand, J.; Smith, E.S.J.; Schwefel, D.; Lapatsina, L.; Poole, K.; Omerbašić, D.; Kozlenkov, A.; Behlke, J.; Lewin, G.R.; Daumke, O. A stomatin dimer modulates the activity of acid-sensing ion channels. *EMBO J.* **2012**, *31*, 3635–3646. [CrossRef] [PubMed]
52. Lapatsina, L.; Jira, J.A.; Smith, E.S.J.; Poole, K.; Kozlenkov, A.; Bilbao, D.; Lewin, G.R.; Heppenstall, P.A. Regulation of ASIC channels by a stomatin/STOML3 complex located in a mobile vesicle pool in sensory neurons. *Open Biol.* **2012**, *2*, 120096. [CrossRef]
53. Moshourab, R.A.; Wetzel, C.; Martinez-Salgado, C.; Lewin, G.R. Stomatin-domain protein interactions with acid-sensing ion channels modulate nociceptor mechanosensitivity. *J. Physiol.* **2013**, *591*, 5555–5574. [CrossRef] [PubMed]
54. Hu, J.; Chiang, L.Y.; Koch, M.; Lewin, G.R. Evidence for a protein tether involved in somatic touch. *EMBO J.* **2010**, *29*, 855–867. [CrossRef]
55. Jin, P.; Jan, L.Y.; Jan, Y.N. Mechanosensitive ion channels: Structural features relevant to mechanotransduction mechanisms. *Annu. Rev. Neurosci.* **2020**, *43*, 207–229. [CrossRef] [PubMed]
56. Enyedi, P.; Czirják, G. Molecular background of leak K^+ currents: Two-pore domain potassium channels. *Physiol. Rev.* **2010**, *90*, 559–605. [CrossRef] [PubMed]
57. Bang, H.; Kim, Y.; Kim, D. TREK-2, a new member of the mechanosensitive tandem-pore K^+ channel family. *J. Biol. Chem.* **2000**, *275*, 17412–17419. [CrossRef]
58. Noël, J.; Zimmermann, K.; Busserolles, J.; Deval, E.; Alloui, A.; Diochot, S.; Guy, N.; Borsotto, M.; Reeh, P.; Eschalier, A.; et al. The mechano-activated K^+ channels TRAAK and TREK-1 control both warm and cold perception. *EMBO J.* **2009**, *28*, 1308–1318. [CrossRef]
59. Pereira, V.; Busserolles, J.; Christin, M.; Devilliers, M.; Poupon, L.; Legha, W.; Alloui, A.; Aissouni, Y.; Bourinet, E.; Lesage, F.; et al. Role of the TREK2 potassium channel in cold and warm thermosensation and in pain perception. *PAIN* **2014**, *155*, 2534–2544. [CrossRef]
60. Brohawn, S.G.; Su, Z.; MacKinnon, R. Mechanosensitivity is mediated directly by the lipid membrane in TRAAK and TREK1 K^+ channels. *Proc. Natl. Acad. Sci. USA* **2014**, *111*, 3614–3619. [CrossRef] [PubMed]
61. Alloui, A.; Zimmermann, K.; Mamet, J.; Duprat, F.; Noel, J.; Chemin, J.; Guy, N.; Blondeau, N.; Voilley, N.; Rubat-Coudert, C.; et al. TREK-1, a K^+ channel involved in polymodal pain perception. *EMBO J.* **2006**, *25*, 2368–2376. [CrossRef] [PubMed]
62. Brohawn, S.G.; del Mármol, J.; MacKinnon, R. Crystal structure of the human K2P TRAAK, a lipid-and mechano-sensitive K^+ ion channel. *Science* **2012**, *335*, 436–441. [CrossRef] [PubMed]

63. Brohawn, S.G.; Campbell, E.B.; MacKinnon, R. Physical mechanism for gating and mechanosensitivity of the human TRAAK K^+ channel. *Nature* **2014**, *516*, 126–130. [CrossRef] [PubMed]
64. Lalevée, N.; Monier, B.; Sénatore, S.; Perrin, L.; Sémériva, M. Control of cardiac rhythm by ORK1, a *Drosophila* two-pore domain potassium channel. *Curr. Biol.* **2006**, *16*, 1502–1508. [CrossRef] [PubMed]
65. Zhang, X.; Zheng, Y.; Ren, Q.; Zhou, H. The involvement of potassium channel ORK1 in short-term memory and sleep in *Drosophila*. *Medicine* **2017**, *96*, e7299. [CrossRef] [PubMed]
66. Wiedmann, F.; Rinné, S.; Donner, B.; Decher, N.; Katus, H.A.; Schmidt, C. Mechanosensitive TREK-1 two-pore-domain potassium (K2P) channels in the cardiovascular system. *Prog. Biophys. Mol. Biol.* **2020**, *159*, 126–135. [CrossRef]
67. Dong, Y.Y.; Pike, A.C.; Mackenzie, A.; McClenaghan, C.; Aryal, P.; Dong, L.; Quigley, A.; Grieben, M.; Goubin, S.; Mukhopadhyay, S.; et al. K2P channel gating mechanisms revealed by structures of TREK-2 and a complex with Prozac. *Science* **2015**, *347*, 1256–1259. [CrossRef] [PubMed]
68. Wang, L.; Zhou, H.; Zhang, M.; Liu, W.; Deng, T.; Zhao, Q.; Li, Y.; Lei, J.; Li, X.; Xiao, B. Structure and mechanogating of the mammalian tactile channel PIEZO2. *Nature* **2019**, *573*, 225–229. [CrossRef] [PubMed]
69. Liang, X.; Howard, J. Structural biology: Piezo senses tension through curvature. *Curr. Biol.* **2018**, *28*, R357–R359. [CrossRef] [PubMed]
70. Geng, J.; Liu, W.; Zhou, H.; Zhang, T.; Wang, L.; Zhang, M.; Li, Y.; Shen, B.; Li, X.; Xiao, B. A Plug-and-Latch Mechanism for Gating the Mechanosensitive Piezo Channel. *Neuron* **2020**, *106*, 438–451. [CrossRef]
71. Ranade, S.S.; Woo, S.H.; Dubin, A.E.; Moshourab, R.A.; Wetzel, C.; Petrus, M.; Mathur, J.; Bégay, V.; Coste, B.; Mainquist, J.; et al. Piezo2 is the major transducer of mechanical forces for touch sensation in mice. *Nature* **2014**, *516*, 121–125. [CrossRef] [PubMed]
72. Wu, Z.; Grillet, N.; Zhao, B.; Cunningham, C.; Harkins-Perry, S.; Coste, B.; Ranade, S.; Zebarjadi, N.; Beurg, M.; Fettiplace, R.; et al. Mechanosensory hair cells express two molecularly distinct mechanotransduction channels. *Nat. Neurosci.* **2017**, *20*, 24–33. [CrossRef] [PubMed]
73. Woo, S.H.; Ranade, S.; Weyer, A.D.; Dubin, A.E.; Baba, Y.; Qiu, Z.; Petrus, M.; Miyamoto, T.; Reddy, K.; Lumpkin, E.A.; et al. Piezo2 is required for Merkel-cell mechanotransduction. *Nature* **2014**, *509*, 622–626. [CrossRef] [PubMed]
74. Coste, B.; Mathur, J.; Schmidt, M.; Earley, T.J.; Ranade, S.; Petrus, M.J.; Dubin, A.E.; Patapoutian, A. Piezo1 and Piezo2 are essential components of distinct mechanically activated cation channels. *Science* **2010**, *330*, 55–60. [CrossRef]
75. Kim, S.E.; Coste, B.; Chadha, A.; Cook, B.; Patapoutian, A. The role of *Drosophila* Piezo in mechanical nociception. *Nature* **2012**, *483*, 209–212. [CrossRef] [PubMed]
76. Bai, X.; Bouffard, J.; Lord, A.; Brugman, K.; Sternberg, P.W.; Cram, E.J.; Golden, A. *Caenorhabditis elegans* PIEZO channel coordinates multiple reproductive tissues to govern ovulation. *Elife* **2020**, *9*, e53603. [CrossRef]
77. Coste, B.; Xiao, B.; Santos, J.S.; Syeda, R.; Grandl, J.; Spencer, K.S.; Kim, S.E.; Schmidt, M.; Mathur, J.; Dubin, A.E.; et al. Piezo proteins are pore-forming subunits of mechanically activated channels. *Nature* **2012**, *483*, 176–181. [CrossRef] [PubMed]
78. Ellefsen, K.L.; Holt, J.R.; Chang, A.C.; Nourse, J.L.; Arulmoli, J.; Mekhdjian, A.H.; Abuwarda, H.; Tombola, F.; Flanagan, L.A.; Dunn, A.R.; et al. Myosin-II mediated traction forces evoke localized Piezo1-dependent Ca^{2+} flickers. *Commun. Biol.* **2019**, *2*, 1–13. [CrossRef] [PubMed]
79. Falleroni, F.; Torre, V.; Cojoc, D. Cell mechanotransduction with piconewton forces applied by optical tweezers. *Front. Cell. Neurosci.* **2018**, *12*, 130. [CrossRef] [PubMed]
80. Wu, J.; Goyal, R.; Grandl, J. Localized force application reveals mechanically sensitive domains of Piezo1. *Nat. Commun.* **2016**, *7*, 12939 . [CrossRef]
81. Jetta, D.; Gottlieb, P.A.; Verma, D.; Sachs, F.; Hua, S.Z. Shear stress-induced nuclear shrinkage through activation of Piezo1 channels in epithelial cells. *J. Cell Sci.* **2019**, *132*. [CrossRef] [PubMed]
82. Wang, S.; Chennupati, R.; Kaur, H.; Iring, A.; Wettschureck, N.; Offermanns, S.; et al. Endothelial cation channel PIEZO1 controls blood pressure by mediating flow-induced ATP release. *J. Clin. Investig.* **2016**, *126*, 4527–4536. [CrossRef] [PubMed]
83. Qi, Y.; Andolfi, L.; Frattini, F.; Mayer, F.; Lazzarino, M.; Hu, J. Membrane stiffening by STOML3 facilitates mechanosensation in sensory neurons. *Nat. Commun.* **2015**, *6*, 8512. [CrossRef] [PubMed]
84. Zhao, Q.; Wu, K.; Geng, J.; Chi, S.; Wang, Y.; Zhi, P.; Zhang, M.; Xiao, B. Ion permeation and mechanotransduction mechanisms of mechanosensitive piezo channels. *Neuron* **2016**, *89*, 1248–1263. [CrossRef] [PubMed]
85. Zheng, W.; Nikolaev, Y.A.; Gracheva, E.O.; Bagriantsev, S.N. Piezo2 integrates mechanical and thermal cues in vertebrate mechanoreceptors. *Proc. Natl. Acad. Sci. USA* **2019**, *116*, 17547–17555. [CrossRef] [PubMed]
86. Cox, C.D.; Bae, C.; Ziegler, L.; Hartley, S.; Nikolova-Krstevski, V.; Rohde, P.R.; Ng, C.A.; Sachs, F.; Gottlieb, P.A.; Martinac, B. Removal of the mechanoprotective influence of the cytoskeleton reveals PIEZO1 is gated by bilayer tension. *Nat. Commun.* **2016**, *7*, 10366. [CrossRef]
87. Retailleau, K.; Duprat, F.; Arhatte, M.; Ranade, S.S.; Peyronnet, R.; Martins, J.R.; Jodar, M.; Moro, C.; Offermanns, S.; Feng, Y.; et al. Piezo1 in smooth muscle cells is involved in hypertension-dependent arterial remodeling. *Cell Rep.* **2015**, *13*, 1161–1171. [CrossRef]
88. Haselwandter, C.A.; MacKinnon, R. Piezo's membrane footprint and its contribution to mechanosensitivity. *Elife* **2018**, *7*, e41968. [CrossRef]

89. Medrano-Soto, A.; Moreno-Hagelsieb, G.; McLaughlin, D.; Ye, Z.S.; Hendargo, K.J.; Saier, M.H., Jr. Bioinformatic characterization of the Anoctamin Superfamily of Ca^{2+}-activated ion channels and lipid scramblases. *PLoS ONE* **2018**, *13*, e0192851. [CrossRef] [PubMed]
90. Jia, Y.; Zhao, Y.; Kusakizako, T.; Wang, Y.; Pan, C.; Zhang, Y.; Nureki, O.; Hattori, M.; Yan, Z. TMC1 and TMC2 proteins are pore-forming subunits of mechanosensitive ion channels. *Neuron* **2020**, *105*, 310–321. [CrossRef] [PubMed]
91. Imtiaz, A.; Maqsood, A.; Rehman, A.U.; Morell, R.J.; Holt, J.R.; Friedman, T.B.; Naz, S. Recessive mutations of TMC1 associated with moderate to severe hearing loss. *Neurogenetics* **2016**, *17*, 115–123. [CrossRef] [PubMed]
92. Kawashima, Y.; Géléoc, G.S.; Kurima, K.; Labay, V.; Lelli, A.; Asai, Y.; Makishima, T.; Wu, D.K.; Della Santina, C.C.; Holt, J.R.; et al. Mechanotransduction in mouse inner ear hair cells requires transmembrane channel–like genes. *J. Clin. Investig.* **2011**, *121*, 4796–4809. [CrossRef]
93. Guo, Y.; Wang, Y.; Zhang, W.; Meltzer, S.; Zanini, D.; Yu, Y.; Li, J.; Cheng, T.; Guo, Z.; Wang, Q.; et al. Transmembrane channel-like (tmc) gene regulates *Drosophila* larval locomotion. *Proc. Natl. Acad. Sci. USA* **2016**, *113*, 7243–7248. [CrossRef] [PubMed]
94. Zhang, Y.V.; Aikin, T.J.; Li, Z.; Montell, C. The basis of food texture sensation in *Drosophila*. *Neuron* **2016**, *91*, 863–877. [CrossRef] [PubMed]
95. Chou, S.W.; Chen, Z.; Zhu, S.; Davis, R.W.; Hu, J.; Liu, L.; Fernando, C.A.; Kindig, K.; Brown, W.C.; Stepanyan, R.; et al. A molecular basis for water motion detection by the mechanosensory lateral line of zebrafish. *Nat. Commun.* **2017**, *8*, 2234. [CrossRef]
96. Chatzigeorgiou, M.; Bang, S.; Hwang, S.W.; Schafer, W.R. tmc-1 encodes a sodium-sensitive channel required for salt chemosensation in *C. elegans*. *Nature* **2013**, *494*, 95–99. [CrossRef] [PubMed]
97. Pan, B.; Akyuz, N.; Liu, X.P.; Asai, Y.; Nist-Lund, C.; Kurima, K.; Derfler, B.H.; György, B.; Limapichat, W.; Walujkar, S.; et al. TMC1 forms the pore of mechanosensory transduction channels in vertebrate inner ear hair cells. *Neuron* **2018**, *99*, 736–753. [CrossRef]
98. Venkatachalam, K.; Montell, C. TRP channels. *Annu. Rev. Biochem.* **2007**, *76*, 387–417. [CrossRef] [PubMed]
99. Himmel, N.J.; Cox, D.N. Transient receptor potential channels: Current perspectives on evolution, structure, function and nomenclature. *Proc. R. Soc. B* **2020**, *287*, 20201309. [CrossRef] [PubMed]
100. Owsianik, G.; Talavera, K.; Voets, T.; Nilius, B. Permeation and selectivity of TRP channels. *Annu. Rev. Physiol.* **2006**, *68*, 685–717. [CrossRef]
101. Nilius, B.; Owsianik, G. The transient receptor potential family of ion channels. *Genome Biol.* **2011**, *12*, 218. [CrossRef] [PubMed]
102. Zhang, W.; Cheng, L.E.; Kittelmann, M.; Li, J.; Petkovic, M.; Cheng, T.; Jin, P.; Guo, Z.; Göpfert, M.C.; Jan, L.Y.; et al. Ankyrin repeats convey force to gate the NOMPC mechanotransduction channel. *Cell* **2015**, *162*, 1391–1403. [CrossRef] [PubMed]
103. Duan, J.; Li, J.; Chen, G.L.; Ge, Y.; Liu, J.; Xie, K.; Peng, X.; Zhou, W.; Zhong, J.; Zhang, Y.; et al. Cryo-EM structure of TRPC5 at 2.8-Å resolution reveals unique and conserved structural elements essential for channel function. *Sci. Adv.* **2019**, *5*, eaaw7935. [CrossRef] [PubMed]
104. Yin, Y.; Wu, M.; Zubcevic, L.; Borschel, W.F.; Lander, G.C.; Lee, S.Y. Structure of the cold-and menthol-sensing ion channel TRPM8. *Science* **2018**, *359*, 237–241. [CrossRef]
105. Viana, F. TRPA1 channels: Molecular sentinels of cellular stress and tissue damage. *J. Physiol.* **2016**, *594*, 4151–4169. [CrossRef] [PubMed]
106. Amini, M.; Wang, H.; Belkacemi, A.; Jung, M.; Bertl, A.; Schlenstedt, G.; Flockerzi, V.; Beck, A. Identification of Inhibitory Ca^{2+} Binding Sites in the Upper Vestibule of the Yeast Vacuolar TRP Channel. *Iscience* **2019**, *11*, 1–12. [CrossRef]
107. Himmel, N.J.; Gray, T.R.; Cox, D.N. Phylogenetics Identifies Two Eumetazoan TRPM Clades and an Eighth TRP Family, TRP Soromelastatin (TRPS). *Mol. Biol. Evol.* **2020**, *37*, 2034–2044. [CrossRef] [PubMed]
108. Delmas, P. Polycystins: Polymodal receptor/ion-channel cellular sensors. *Pflügers Archiv* **2005**, *451*, 264–276. [CrossRef] [PubMed]
109. Eijkelkamp, N.; Quick, K.; Wood, J.N. Transient receptor potential channels and mechanosensation. *Annu. Rev. Neurosci.* **2013**, *36*, 519–546. [CrossRef]
110. Edwards-Jorquera, S.S.; Bosveld, F.; Bellaïche, Y.A.; Lennon-Duménil, A.M.; Glavic, Á. Trpml controls actomyosin contractility and couples migration to phagocytosis in fly macrophages. *J. Cell Biol.* **2020**, *219*, e201905228. [CrossRef] [PubMed]
111. Effertz, T.; Wiek, R.; Göpfert, M.C. NompC TRP channel is essential for *Drosophila* sound receptor function. *Curr. Biol.* **2011**, *21*, 592–597. [CrossRef]
112. Lehnert, B.P.; Baker, A.E.; Gaudry, Q.; Chiang, A.S.; Wilson, R.I. Distinct roles of TRP channels in auditory transduction and amplification in *Drosophila*. *Neuron* **2013**, *77*, 115–128. [CrossRef]
113. Sexton, J.E.; Desmonds, T.; Quick, K.; Taylor, R.; Abramowitz, J.; Forge, A.; Kros, C.J.; Birnbaumer, L.; Wood, J.N. The contribution of TRPC1, TRPC3, TRPC5 and TRPC6 to touch and hearing. *Neurosci. Lett.* **2016**, *610*, 36–42. [CrossRef] [PubMed]
114. Quick, K.; Zhao, J.; Eijkelkamp, N.; Linley, J.E.; Rugiero, F.; Cox, J.J.; Raouf, R.; Gringhuis, M.; Sexton, J.E.; Abramowitz, J.; et al. TRPC3 and TRPC6 are essential for normal mechanotransduction in subsets of sensory neurons and cochlear hair cells. *Open Biol.* **2012**, *2*, 120068. [CrossRef] [PubMed]
115. Yan, Z.; Zhang, W.; He, Y.; Gorczyca, D.; Xiang, Y.; Cheng, L.E.; Meltzer, S.; Jan, L.Y.; Jan, Y.N. *Drosophila* NOMPC is a mechanotransduction channel subunit for gentle-touch sensation. *Nature* **2013**, *493*, 221–225. [CrossRef] [PubMed]
116. Zhang, M.; Li, X.; Zheng, H.; Wen, X.; Chen, S.; Ye, J.; Tang, S.; Yao, F.; Li, Y.; Yan, Z. Brv1 is required for *Drosophila* larvae to sense gentle touch. *Cell Rep.* **2018**, *23*, 23–31. [CrossRef]

117. Garrison, S.R.; Dietrich, A.; Stucky, C.L. TRPC1 contributes to light-touch sensation and mechanical responses in low-threshold cutaneous sensory neurons. *J. Neurophysiol.* **2012**, *107*, 913–922. [CrossRef]
118. Kindt, K.S.; Viswanath, V.; Macpherson, L.; Quast, K.; Hu, H.; Patapoutian, A.; Schafer, W.R. *Caenorhabditis elegans* TRPA-1 functions in mechanosensation. *Nat. Neurosci.* **2007**, *10*, 568–577. [CrossRef]
119. Lau, O.C.; Shen, B.; Wong, C.O.; Tjong, Y.W.; Lo, C.Y.; Wang, H.C.; Huang, Y.; Yung, W.H.; Chen, Y.C.; Fung, M.L.; et al. TRPC5 channels participate in pressure-sensing in aortic baroreceptors. *Nat. Commun.* **2016**, *7*, 11947. [CrossRef] [PubMed]
120. Glazebrook, P.A.; Schilling, W.P.; Kunze, D.L. TRPC channels as signal transducers. *Pflügers Archiv* **2005**, *451*, 125–130. [CrossRef] [PubMed]
121. Li, W.; Feng, Z.; Sternberg, P.W.; Xu, X.S. A C. elegans stretch receptor neuron revealed by a mechanosensitive TRP channel homologue. *Nature* **2006**, *440*, 684–687. [CrossRef]
122. Kang, L.; Gao, J.; Schafer, W.R.; Xie, Z.; Xu, X.S. *C. elegans* TRP family protein TRP-4 is a pore-forming subunit of a native mechanotransduction channel. *Neuron* **2010**, *67*, 381–391. [CrossRef] [PubMed]
123. Yeon, J.; Kim, J.; Kim, D.Y.; Kim, H.; Kim, J.; Du, E.J.; Kang, K.; Lim, H.H.; Moon, D.; Kim, K. A sensory-motor neuron type mediates proprioceptive coordination of steering in *C. elegans* via two TRPC channels. *PLoS Biol.* **2018**, *16*, e2004929. [CrossRef] [PubMed]
124. Kwan, K.Y.; Allchorne, A.J.; Vollrath, M.A.; Christensen, A.P.; Zhang, D.S.; Woolf, C.J.; Corey, D.P. TRPA1 contributes to cold, mechanical, and chemical nociception but is not essential for hair-cell transduction. *Neuron* **2006**, *50*, 277–289. [CrossRef]
125. Hwang, R.Y.; Stearns, N.A.; Tracey, W.D. The ankyrin repeat domain of the TRPA protein painless is important for thermal nociception but not mechanical nociception. *PLoS ONE* **2012**, *7*, e30090. [CrossRef]
126. Zhang, X.F.; Chen, J.; Faltynek, C.R.; Moreland, R.B.; Neelands, T.R. Transient receptor potential A1 mediates an osmotically activated ion channel. *Eur. J. Neurosci.* **2008**, *27*, 605–611. [CrossRef]
127. Liu, Y.S.; Liu, Y.A.; Huang, C.J.; Yen, M.H.; Tseng, C.T.; Chien, S.; Lee, O.K. Mechanosensitive TRPM7 mediates shear stress and modulates osteogenic differentiation of mesenchymal stromal cells through Osterix pathway. *Sci. Rep.* **2015**, *5*, 16522. [CrossRef]
128. Hardie, R.C.; Franze, K. Photomechanical responses in *Drosophila* photoreceptors. *Science* **2012**, *338*, 260–263. [CrossRef] [PubMed]
129. Christensen, A.P.; Corey, D.P. TRP channels in mechanosensation: Direct or indirect activation? *Nat. Rev. Neurosci.* **2007**, *8*, 510–521. [CrossRef] [PubMed]
130. Liu, C.; Montell, C. Forcing open TRP channels: Mechanical gating as a unifying activation mechanism. *Biochem. Biophys. Res. Commun.* **2015**, *460*, 22–25. [CrossRef] [PubMed]
131. Nikolaev, Y.A.; Cox, C.D.; Ridone, P.; Rohde, P.R.; Cordero-Morales, J.F.; Vásquez, V.; Laver, D.R.; Martinac, B. Mammalian TRP ion channels are insensitive to membrane stretch. *J. Cell Sci.* **2019**, *132*, jcs238360. [CrossRef]
132. Nilius, B. Polycystins under pressure. *Cell* **2009**, *139*, 466–467. [CrossRef] [PubMed]
133. Sharif-Naeini, R.; Folgering, J.H.; Bichet, D.; Duprat, F.; Lauritzen, I.; Arhatte, M.; Jodar, M.; Dedman, A.; Chatelain, F.C.; Schulte, U.; et al. Polycystin-1 and-2 dosage regulates pressure sensing. *Cell* **2009**, *139*, 587–596. [CrossRef] [PubMed]
134. Pratt, S.J.; Lee, R.M.; Chang, K.T.; Hernández-Ochoa, E.O.; Annis, D.A.; Ory, E.C.; Thompson, K.N.; Bailey, P.C.; Mathias, T.J.; Ju, J.A.; et al. Mechanoactivation of NOX2-generated ROS elicits persistent TRPM8 Ca^{2+} signals that are inhibited by oncogenic KRas. *Proc. Natl. Acad. Sci. USA* **2020**, *117*, 26008–26019. [CrossRef]
135. Prager-Khoutorsky, M.; Khoutorsky, A.; Bourque, C.W. Unique interweaved microtubule scaffold mediates osmosensory transduction via physical interaction with TRPV1. *Neuron* **2014**, *83*, 866–878. [CrossRef] [PubMed]
136. Suzuki, M.; Mizuno, A.; Kodaira, K.; Imai, M. Impaired pressure sensation in mice lacking TRPV4. *J. Biol. Chem.* **2003**, *278*, 22664–22668. [CrossRef]
137. Gao, F.; Yang, Z.; Jacoby, R.A.; Wu, S.M.; Pang, J.J. The expression and function of TRPV4 channels in primate retinal ganglion cells and bipolar cells. *Cell Death Dis.* **2019**, *10*, 1–12. [CrossRef]
138. Strotmann, R.; Harteneck, C.; Nunnenmacher, K.; Schultz, G.; Plant, T.D. OTRPC4, a nonselective cation channel that confers sensitivity to extracellular osmolarity. *Nat. Cell Biol.* **2000**, *2*, 695–702. [CrossRef] [PubMed]
139. Maroto, R.; Raso, A.; Wood, T.G.; Kurosky, A.; Martinac, B.; Hamill, O.P. TRPC1 forms the stretch-activated cation channel in vertebrate cells. *Nat. Cell Biol.* **2005**, *7*, 179–185. [CrossRef] [PubMed]
140. Shen, B.; Wong, C.O.; Lau, O.C.; Woo, T.; Bai, S.; Huang, Y.; Yao, X. Plasma membrane mechanical stress activates TRPC5 channels. *PLoS ONE* **2015**, *10*, e0122227. [CrossRef]
141. Yamaguchi, Y.; Iribe, G.; Nishida, M.; Naruse, K. Role of TRPC3 and TRPC6 channels in the myocardial response to stretch: Linking physiology and pathophysiology. *Prog. Biophys. Mol. Biol.* **2017**, *130*, 264–272. [CrossRef] [PubMed]
142. Wilson, C.; Dryer, S.E. A mutation in TRPC6 channels abolishes their activation by hypoosmotic stretch but does not affect activation by diacylglycerol or G protein signaling cascades. *Am. J. Physiol.-Ren. Physiol.* **2014**, *306*, F1018–F1025. [CrossRef] [PubMed]
143. Spassova, M.A.; Hewavitharana, T.; Xu, W.; Soboloff, J.; Gill, D.L. A common mechanism underlies stretch activation and receptor activation of TRPC6 channels. *Proc. Natl. Acad. Sci. USA* **2006**, *103*, 16586–16591. [CrossRef]
144. Dyachenko, V.; Husse, B.; Rueckschloss, U.; Isenberg, G. Mechanical deformation of ventricular myocytes modulates both TRPC6 and Kir2. 3 channels. *Cell Calcium* **2009**, *45*, 38–54. [CrossRef] [PubMed]
145. Anderson, M.; Kim, E.Y.; Hagmann, H.; Benzing, T.; Dryer, S.E. Opposing effects of podocin on the gating of podocyte TRPC6 channels evoked by membrane stretch or diacylglycerol. *Am. J. Physiol.-Cell Physiol.* **2013**, *305*, C276–C289. [CrossRef] [PubMed]

146. Numata, T.; Shimizu, T.; Okada, Y. Direct mechano-stress sensitivity of TRPM7 channel. *Cell. Physiol. Biochem.* **2007**, *19*, 1–8. [CrossRef] [PubMed]
147. Morita, H.; Honda, A.; Inoue, R.; Ito, Y.; Abe, K.; Nelson, M.T.; Brayden, J.E. Membrane stretch-induced activation of a TRPM4-like nonselective cation channel in cerebral artery myocytes. *J. Pharmacol. Sci.* **2007**, *103*, 417–426. [CrossRef] [PubMed]
148. Nauli, S.M.; Alenghat, F.J.; Luo, Y.; Williams, E.; Vassilev, P.; Li, X.; Elia, A.E.; Lu, W.; Brown, E.M.; Quinn, S.J.; et al. Polycystins 1 and 2 mediate mechanosensation in the primary cilium of kidney cells. *Nat. Genet.* **2003**, *33*, 129–137. [CrossRef] [PubMed]
149. Loukin, S.; Zhou, X.; Su, Z.; Saimi, Y.; Kung, C. Wild-type and brachyolmia-causing mutant TRPV4 channels respond directly to stretch force. *J. Biol. Chem.* **2010**, *285*, 27176–27181. [CrossRef] [PubMed]
150. Mopharty, L.; Zygmunt, P.M. Human TRPA1 is an inherently mechanosensitive bilayer-gated ion channel. *Cell Calcium* **2020**, *91*, 102255.
151. Sun, Y.; Liu, L.; Ben-Shahar, Y.; Jacobs, J.S.; Eberl, D.F.; Welsh, M.J. TRPA channels distinguish gravity sensing from hearing in Johnston's organ. *Proc. Natl. Acad. Sci. USA* **2009**, *106*, 13606–13611. [CrossRef]
152. Gottlieb, P.; Folgering, J.; Maroto, R.; Raso, A.; Wood, T.G.; Kurosky, A.; Bowman, C.; Bichet, D.; Patel, A.; Sachs, F.; et al. Revisiting TRPC1 and TRPC6 mechanosensitivity. *Pflügers Archiv-Eur. J. Physiol.* **2008**, *455*, 1097–1103. [CrossRef] [PubMed]
153. Servin-Vences, M.R.; Moroni, M.; Lewin, G.R.; Poole, K. Direct measurement of TRPV4 and PIEZO1 activity reveals multiple mechanotransduction pathways in chondrocytes. *Elife* **2017**, *6*, e21074. [CrossRef]
154. Constantine, M.; Liew, C.K.; Lo, V.; Macmillan, A.; Cranfield, C.G.; Sunde, M.; Whan, R.; Graham, R.M.; Martinac, B. Heterologously-expressed and liposome-reconstituted human transient receptor potential melastatin 4 channel (TRPM4) is a functional tetramer. *Sci. Rep.* **2016**, *6*, 19352. [CrossRef] [PubMed]
155. Geffeney, S.L.; Cueva, J.G.; Glauser, D.A.; Doll, J.C.; Lee, T.H.C.; Montoya, M.; Karania, S.; Garakani, A.M.; Pruitt, B.L.; Goodman, M.B. DEG/ENaC but not TRP channels are the major mechanoelectrical transduction channels in a *C. elegans* nociceptor. *Neuron* **2011**, *71*, 845–857. [CrossRef] [PubMed]
156. Yan, C.; Wang, F.; Peng, Y.; Williams, C.R.; Jenkins, B.; Wildonger, J.; Kim, H.J.; Perr, J.B.; Vaughan, J.C.; Kern, M.E.; et al. Microtubule acetylation is required for mechanosensation in *Drosophila*. *Cell Rep.* **2018**, *25*, 1051–1065. [CrossRef] [PubMed]
157. Page, A.J.; Brierley, S.M.; Martin, C.M.; Price, M.P.; Symonds, E.; Butler, R.; Wemmie, J.A.; Blackshaw, L. Different contributions of ASIC channels 1a, 2, and 3 in gastrointestinal mechanosensory function. *Gut* **2005**, *54*, 1408–1415. [CrossRef] [PubMed]
158. Poole, K.; Herget, R.; Lapatsina, L.; Ngo, H.D.; Lewin, G.R. Tuning Piezo ion channels to detect molecular-scale movements relevant for fine touch. *Nat. Commun.* **2014**, *5*, 3520. [CrossRef]
159. Yue, X.; Zhao, J.; Li, X.; Fan, Y.; Duan, D.; Zhang, X.; Zou, W.; Sheng, Y.; Zhang, T.; Yang, Q.; et al. TMC proteins modulate egg laying and membrane excitability through a background leak conductance in *C. elegans*. *Neuron* **2018**, *97*, 571–585. [CrossRef]
160. Walker, R.G.; Willingham, A.T.; Zuker, C.S. A *Drosophila* mechanosensory transduction channel. *Science* **2000**, *287*, 2229–2234. [CrossRef] [PubMed]
161. Liang, X.; Madrid, J.; Gärtner, R.; Verbavatz, J.M.; Schiklenk, C.; Wilsch-Bräuninger, M.; Bogdanova, A.; Stenger, F.; Voigt, A.; Howard, J. A NOMPC-dependent membrane-microtubule connector is a candidate for the gating spring in fly mechanoreceptors. *Curr. Biol.* **2013**, *23*, 755–763. [CrossRef] [PubMed]
162. Jin, P.; Bulkley, D.; Guo, Y.; Zhang, W.; Guo, Z.; Huynh, W.; Wu, S.; Meltzer, S.; Cheng, T.; Jan, L.Y.; et al. Electron cryo-microscopy structure of the mechanotransduction channel NOMPC. *Nature* **2017**, *547*, 118–122. [CrossRef]
163. Sun, L.; Gao, Y.; He, J.; Cui, L.; Meissner, J.; Verbavatz, J.M.; Li, B.; Feng, X.; Liang, X. Ultrastructural organization of NompC in the mechanoreceptive organelle of *Drosophila* campaniform mechanoreceptors. *Proc. Natl. Acad. Sci. USA* **2019**, *116*, 7343–7352. [CrossRef] [PubMed]
164. Sidi, S.; Friedrich, R.W.; Nicolson, T. NompC TRP channel required for vertebrate sensory hair cell mechanotransduction. *Science* **2003**, *301*, 96–99. [CrossRef] [PubMed]
165. Zhang, Z.; Kindrat, A.N.; Sharif-Naeini, R.; Bourque, C.W. Actin filaments mediate mechanical gating during osmosensory transduction in rat supraoptic nucleus neurons. *J. Neurosci.* **2007**, *27*, 4008–4013. [CrossRef]
166. Zaelzer, C.; Hua, P.; Prager-Khoutorsky, M.; Ciura, S.; Voisin, D.L.; Liedtke, W.; Bourque, C.W. ΔN-TRPV1: A molecular co-detector of body temperature and osmotic stress. *Cell Rep.* **2015**, *13*, 23–30. [CrossRef] [PubMed]
167. Ciura, S.; Bourque, C.W. Transient receptor potential vanilloid 1 is required for intrinsic osmoreception in organum vasculosum lamina terminalis neurons and for normal thirst responses to systemic hyperosmolality. *J. Neurosci.* **2006**, *26*, 9069–9075. [CrossRef] [PubMed]
168. Ciura, S.; Liedtke, W.; Bourque, C.W. Hypertonicity sensing in organum vasculosum lamina terminalis neurons: A mechanical process involving TRPV1 but not TRPV4. *J. Neurosci.* **2011**, *31*, 14669–14676. [CrossRef] [PubMed]
169. Mihara, H.; Boudaka, A.; Shibasaki, K.; Yamanaka, A.; Sugiyama, T.; Tominaga, M. Involvement of TRPV2 activation in intestinal movement through nitric oxide production in mice. *J. Neurosci.* **2010**, *30*, 16536–16544. [CrossRef]
170. Suzuki, M.; Watanabe, Y.; Oyama, Y.; Mizuno, A.; Kusano, E.; Hirao, A.; Ookawara, S. Localization of mechanosensitive channel TRPV4 in mouse skin. *Neurosci. Lett.* **2003**, *353*, 189–192. [CrossRef] [PubMed]
171. Ryskamp, D.A.; Jo, A.O.; Frye, A.M.; Vazquez-Chona, F.; MacAulay, N.; Thoreson, W.B.; Križaj, D. Swelling and eicosanoid metabolites differentially gate TRPV4 channels in retinal neurons and glia. *J. Neurosci.* **2014**, *34*, 15689–15700. [CrossRef]
172. Lakk, M.; Young, D.; Baumann, J.M.; Jo, A.O.; Hu, H.; Križaj, D. Polymodal TRPV1 and TRPV4 sensors colocalize but do not functionally interact in a subpopulation of mouse retinal ganglion cells. *Front. Cell. Neurosci.* **2018**, *12*, 353. [CrossRef] [PubMed]

173. Liedtke, W.; Choe, Y.; Martí-Renom, M.A.; Bell, A.M.; Denis, C.S.; Hudspeth, A.; Friedman, J.M.; Heller, S.; et al. Vanilloid receptor–related osmotically activated channel (VR-OAC), a candidate vertebrate osmoreceptor. *Cell* **2000**, *103*, 525–535. [CrossRef]
174. Richter, F.; von Banchet, G.S.; Schaible, H.G. Transient Receptor Potential vanilloid 4 ion channel in C-fibres is involved in mechanonociception of the normal and inflamed joint. *Sci. Rep.* **2019**, *9*, 10928 . [CrossRef] [PubMed]
175. Upadhyay, A.; Pisupati, A.; Jegla, T.; Crook, M.; Mickolajczyk, K.J.; Shorey, M.; Rohan, L.E.; Billings, K.A.; Rolls, M.M.; Hancock, W.O.; et al. Nicotinamide is an endogenous agonist for a *C. elegans* TRPV OSM-9 and OCR-4 channel. *Nat. Commun.* **2016**, *7*, 13135. [CrossRef]
176. Tobin, D.M.; Madsen, D.M.; Kahn-Kirby, A.; Peckol, E.L.; Moulder, G.; Barstead, R.; Maricq, A.V.; Bargmann, C.I. Combinatorial expression of TRPV channel proteins defines their sensory functions and subcellular localization in *C. elegans* neurons. *Neuron* **2002**, *35*, 307–318. [CrossRef]
177. Kahn-Kirby, A.H.; Dantzker, J.L.; Apicella, A.J.; Schafer, W.R.; Browse, J.; Bargmann, C.I.; Watts, J.L. Specific polyunsaturated fatty acids drive TRPV-dependent sensory signaling in vivo. *Cell* **2004**, *119*, 889–900. [CrossRef]
178. Montell, C. *Drosophila* TRP channels. *Pflügers Archiv* **2005**, *451*, 19–28. [CrossRef]
179. O'Neil, R.G.; Heller, S. The mechanosensitive nature of TRPV channels. *Pflügers Archiv* **2005**, *451*, 193–203. [CrossRef] [PubMed]
180. Gong, Z.; Son, W.; Chung, Y.D.; Kim, J.; Shin, D.W.; McClung, C.A.; Lee, Y.; Lee, H.W.; Chang, D.J.; Kaang, B.K.; et al. Two interdependent TRPV channel subunits, inactive and Nanchung, mediate hearing in *Drosophila*. *J. Neurosci.* **2004**, *24*, 9059–9066. [CrossRef] [PubMed]
181. Clark, K.; Langeslag, M.; Van Leeuwen, B.; Ran, L.; Ryazanov, A.G.; Figdor, C.G.; Moolenaar, W.H.; Jalink, K.; Van Leeuwen, F.N. TRPM7, a novel regulator of actomyosin contractility and cell adhesion. *EMBO J.* **2006**, *25*, 290–301. [CrossRef] [PubMed]
182. Langeslag, M.; Clark, K.; Moolenaar, W.H.; van Leeuwen, F.N.; Jalink, K. Activation of TRPM7 channels by phospholipase C-coupled receptor agonists. *J. Biol. Chem.* **2007**, *282*, 232–239. [CrossRef] [PubMed]
183. Wei, C.; Wang, X.; Chen, M.; Ouyang, K.; Song, L.S.; Cheng, H. Calcium flickers steer cell migration. *Nature* **2009**, *457*, 901–905. [CrossRef]
184. Bernhardt, M.L.; Stein, P.; Carvacho, I.; Krapp, C.; Ardestani, G.; Mehregan, A.; Umbach, D.M.; Bartolomei, M.S.; Fissore, R.A.; Williams, C.J. TRPM7 and CaV3. 2 channels mediate Ca^{2+} influx required for egg activation at fertilization. *Proc. Natl. Acad. Sci. USA* **2018**, *115*, E10370–E10378. [CrossRef] [PubMed]
185. O'Hagan, R.; Wang, J.; Barr, M.M. Mating behavior, male sensory cilia, and polycystins in *Caenorhabditis elegans*. *Semin. Cell Dev. Biol.* **2014**, *33*, 25–33. [CrossRef]
186. Gianmarchi, A.; Delmas, P. Activation Mechanisms and Functional Roles of TRPP2 Cation Channels. In *TRP Ion Channel Function in Sensory Transduction and Cellular Signaling Cascades*; Liedtke, W., Heller, S., Eds.; CRC Press/Taylor & Francis: Boca Raton, FL, USA, 2007; Chapter 14.
187. Lam, R.M.; Chesler, A.T. Shear elegance: A novel screen uncovers a mechanosensitive GPCR. *J. Gen. Physiol.* **2018**, *150*, 907–910. [CrossRef]
188. Chachisvilis, M.; Zhang, Y.L.; Frangos, J.A. G protein-coupled receptors sense fluid shear stress in endothelial cells. *Proc. Natl. Acad. Sci. USA* **2006**, *103*, 15463–15468. [CrossRef] [PubMed]
189. Zou, Y.; Akazawa, H.; Qin, Y.; Sano, M.; Takano, H.; Minamino, T.; Makita, N.; Iwanaga, K.; Zhu, W.; Kudoh, S.; et al. Mechanical stress activates angiotensin II type 1 receptor without the involvement of angiotensin II. *Nat. Cell Biol.* **2004**, *6*, 499–506. [CrossRef]
190. Xu, J.; Mathur, J.; Vessières, E.; Hammack, S.; Nonomura, K.; Favre, J.; Grimaud, L.; Petrus, M.; Francisco, A.; Li, J.; et al. GPR68 senses flow and is essential for vascular physiology. *Cell* **2018**, *173*, 762–775. [CrossRef] [PubMed]
191. Erdogmus, S.; Storch, U.; Danner, L.; Becker, J.; Winter, M.; Ziegler, N.; Wirth, A.; Offermanns, S.; Hoffmann, C.; Gudermann, T.; et al. Helix 8 is the essential structural motif of mechanosensitive GPCRs. *Nat. Commun.* **2019**, *10*, 5784. [CrossRef] [PubMed]
192. Franz, F.; Daday, C.; Gräter, F. Advances in molecular simulations of protein mechanical properties and function. *Curr. Opin. Struct. Biol.* **2020**, *61*, 132–138. [CrossRef]
193. Cox, C.D.; Bavi, N.; Martinac, B. Biophysical principles of ion-channel-mediated mechanosensory transduction. *Cell Rep.* **2019**, *29*, 1–12. [CrossRef] [PubMed]
194. Wang, Q.; Corey, R.A.; Hedger, G.; Aryal, P.; Grieben, M.; Nasrallah, C.; Baronina, A.; Pike, A.C.; Shi, J.; Carpenter, E.P.; et al. Lipid interactions of a ciliary membrane TRP channel: Simulation and structural studies of polycystin-2. *Structure* **2020**, *28*, 169–184. [CrossRef] [PubMed]
195. Duncan, A.L.; Corey, R.A.; Sansom, M.S. Defining how multiple lipid species interact with inward rectifier potassium (Kir2) channels. *Proc. Natl. Acad. Sci. USA* **2020**, *117*, 7803–7813. [CrossRef] [PubMed]
196. Duncan, A.L.; Song, W.; Sansom, M.S. Lipid-dependent regulation of ion channels and G protein–coupled receptors: Insights from structures and simulations. *Annu. Rev. Pharmacol. Toxicol.* **2020**, *60*, 31–50. [CrossRef] [PubMed]
197. Hansen, S.B.; Tao, X.; MacKinnon, R. Structural basis of PIP 2 activation of the classical inward rectifier K^+ channel Kir2. 2. *Nature* **2011**, *477*, 495–498. [CrossRef]
198. Guo, Y.R.; MacKinnon, R. Structure-based membrane dome mechanism for Piezo mechanosensitivity. *Elife* **2017**, *6*, e33660. [CrossRef] [PubMed]
199. Grieben, M.; Pike, A.C.; Shintre, C.A.; Venturi, E.; El-Ajouz, S.; Tessitore, A.; Shrestha, L.; Mukhopadhyay, S.; Mahajan, P.; Chalk, R.; et al. Structure of the polycystic kidney disease TRP channel Polycystin-2 (PC2). *Nat. Struct. Mol. Biol.* **2017**, *24*, 114–122. [CrossRef] [PubMed]

200. Aryal, P.; Jarerattanachat, V.; Clausen, M.V.; Schewe, M.; McClenaghan, C.; Argent, L.; Conrad, L.J.; Dong, Y.Y.; Pike, A.C.; Carpenter, E.P.; et al. Bilayer-mediated structural transitions control mechanosensitivity of the TREK-2 K2P channel. *Structure* **2017**, *25*, 708–718. [CrossRef] [PubMed]
201. Nematian-Ardestani, E.; Jarerattanachat, V.; Aryal, P.; Sansom, M.S.; Tucker, S.J. The effects of stretch activation on ionic selectivity of the TREK-2 K2P K^+ channel. *Channels* **2017**, *11*, 482–486. [CrossRef] [PubMed]
202. Clausen, M.V.; Jarerattanachat, V.; Carpenter, E.P.; Sansom, M.S.; Tucker, S.J. Asymmetric mechanosensitivity in a eukaryotic ion channel. *Proc. Natl. Acad. Sci. USA* **2017**, *114*, E8343–E8351. [CrossRef] [PubMed]
203. Brennecke, J.T.; de Groot, B.L. Mechanism of mechanosensitive gating of the TREK-2 potassium channel. *Biophys. J.* **2018**, *114*, 1336–1343. [CrossRef]
204. Kocer, A. Mechanisms of mechanosensing—Mechanosensitive channels, function and re-engineering. *Curr. Opin. Chem. Biol.* **2015**, *29*, 120–127. [CrossRef]
205. Ocello, R.; Furini, S.; Lugli, F.; Recanatini, M.; Domene, C.; Masetti, M. Conduction and Gating Properties of the TRAAK Channel from Molecular Dynamics Simulations with Different Force Fields. *J. Chem. Inf. Model.* **2020**, *60*, 6532–6543. [CrossRef]
206. Masetti, M.; Berti, C.; Ocello, R.; Di Martino, G.P.; Recanatini, M.; Fiegna, C.; Cavalli, A. Multiscale simulations of a two-pore potassium channel. *J. Chem. Theory Comput.* **2016**, *12*, 5681–5687. [CrossRef] [PubMed]
207. Stansfeld, P.J.; Sansom, M.S. From coarse grained to atomistic: A serial multiscale approach to membrane protein simulations. *J. Chem. Theory Comput.* **2011**, *7*, 1157–1166. [CrossRef] [PubMed]
208. De Vecchis, D.; Beech, D.J.; Kalli, A.C. Molecular principles of Piezo1 activation by increased membrane tension. *bioRxiv* **2019**. [CrossRef]
209. Tang, Y.; Yoo, J.; Yethiraj, A.; Cui, Q.; Chen, X. Mechanosensitive channels: Insights from continuum-based simulations. *Cell Biochem. Biophys.* **2008**, *52*, 1. [CrossRef] [PubMed]
210. Bavi, O.; Vossoughi, M.; Naghdabadi, R.; Jamali, Y. The combined effect of hydrophobic mismatch and bilayer local bending on the regulation of mechanosensitive ion channels. *PLoS ONE* **2016**, *11*, e0150578. [CrossRef] [PubMed]
211. Vanegas, J.M.; Torres-Sánchez, A.; Arroyo, M. Importance of force decomposition for local stress calculations in biomembrane molecular simulations. *J. Chem. Theory Comput.* **2014**, *10*, 691–702. [CrossRef] [PubMed]
212. Torres-Sánchez, A.; Vanegas, J.M.; Arroyo, M. Examining the mechanical equilibrium of microscopic stresses in molecular simulations. *Phys. Rev. Lett.* **2015**, *114*, 258102. [CrossRef]
213. Eastwood, A.L.; Sanzeni, A.; Petzold, B.C.; Park, S.J.; Vergassola, M.; Pruitt, B.L.; Goodman, M.B. Tissue mechanics govern the rapidly adapting and symmetrical response to touch. *Proc. Natl. Acad. Sci. USA* **2015**, *112*, E6955–E6963. [CrossRef] [PubMed]
214. Nikolic, K.; Loizu, J.; Degenaar, P.; Toumazou, C. A stochastic model of the single photon response in *Drosophila* photoreceptors. *Integr. Biol.* **2010**, *2*, 354–370. [CrossRef] [PubMed]
215. Thomas, P.J.; Eckford, A.W. Capacity of a simple intercellular signal transduction channel. *IEEE Trans. Inf. Theory* **2016**, *62*, 7358–7382. [CrossRef]
216. Jérusalem, A.; García-Grajales, J.A.; Merchán-Pérez, A.; Peña, J.M. A computational model coupling mechanics and electrophysiology in spinal cord injury. *Biomech. Model. Mechanobiol.* **2014**, *13*, 883–896. [CrossRef] [PubMed]
217. Tian, J.; Huang, G.; Lin, M.; Qiu, J.; Sha, B.; Lu, T.J.; Xu, F. A mechanoelectrical coupling model of neurons under stretching. *J. Mech. Behav. Biomed. Mater.* **2019**, *93*, 213–221. [CrossRef] [PubMed]
218. Engelbrecht, J.; Peets, T.; Tamm, K. Electromechanical coupling of waves in nerve fibres. *Biomech. Model. Mechanobiol.* **2018**, *17*, 1771–1783. [CrossRef]
219. Sripati, A.P.; Bensmaia, S.J.; Johnson, K.O. A continuum mechanical model of mechanoreceptive afferent responses to indented spatial patterns. *J. Neurophysiol.* **2006**, *95*, 3852–3864. [CrossRef]
220. Lesniak, D.R.; Gerling, G.J. Predicting SA-I mechanoreceptor spike times with a skin-neuron model. *Math. Biosci.* **2009**, *220*, 15–23. [CrossRef]
221. Gerling, G.J.; Wan, L.; Hoffman, B.U.; Wang, Y.; Lumpkin, E.A. Computation predicts rapidly adapting mechanotransduction currents cannot account for tactile encoding in Merkel cell-neurite complexes. *PLoS Comput. Biol.* **2018**, *14*, e1006264. [CrossRef]
222. Quindlen, J.C.; Stolarski, H.K.; Johnson, M.D.; Barocas, V.H. A multiphysics model of the Pacinian corpuscle. *Integr. Biol.* **2016**, *8*, 1111–1125. [CrossRef] [PubMed]
223. Sanzeni, A.; Katta, S.; Petzold, B.; Pruitt, B.L.; Goodman, M.B.; Vergassola, M. Somatosensory neurons integrate the geometry of skin deformation and mechanotransduction channels to shape touch sensing. *Elife* **2019**, *8*, e43226. [CrossRef]
224. Chiodo, L.; Malliavin, T.; Maragliano, L.; Cottone, G. A possible desensitized state conformation of the human $\alpha 7$ nicotinic receptor: A molecular dynamics study. *Biophys. Chem.* **2017**, *229*, 99–109. [CrossRef]
225. Cottone, G.; Chiodo, L.; Maragliano, L. Thermodynamics and kinetics of ion permeation in wild-type and mutated open active conformation of the human $\alpha 7$ nicotinic receptor. *J. Chem. Inf. Model.* **2020**, *60*, 5045–5056. [CrossRef] [PubMed]
226. Loppini, A.; Braun, M.; Filippi, S.; Pedersen, M.G. Mathematical modeling of gap junction coupling and electrical activity in human β-cells. *Phys. Biol.* **2015**, *12*, 066002. [CrossRef] [PubMed]
227. Bini, D.; Cherubini, C.; Filippi, S. Heat transfer in Fitzhugh-Nagumo models. *Phys. Rev. E* **2006**, *74*, 041905. [CrossRef] [PubMed]
228. Nestola, M.G.C.; Faggiano, E.; Vergara, C.; Lancellotti, R.M.; Ippolito, S.; Antona, C.; Filippi, S.; Quarteroni, A.; Scrofani, R. Computational comparison of aortic root stresses in presence of stentless and stented aortic valve bio-prostheses. *Comput. Methods Biomech. Biomed. Eng.* **2017**, *20*, 171–181. [CrossRef] [PubMed]

229. Bianchi, D.; Monaldo, E.; Gizzi, A.; Marino, M.; Filippi, S.; Vairo, G. A FSI computational framework for vascular physiopathology: A novel flow-tissue multiscale strategy. *Med. Eng. Phys.* **2017**, *47*, 25–37. [CrossRef] [PubMed]
230. Gizzi, A.; Cherubini, C.; Pomella, N.; Persichetti, P.; Vasta, M.; Filippi, S. Computational modeling and stress analysis of columellar biomechanics. *J. Mech. Behav. Biomed. Mater.* **2012**, *15*, 46–58. [CrossRef]
231. Gizzi, A.; Ruiz-Baier, R.; Rossi, S.; Laadhari, A.; Cherubini, C.; Filippi, S. A three-dimensional continuum model of active contraction in single cardiomyocytes. In *Modeling the Heart and the Circulatory System*; Springer: Cham, Switzerland, 2015; pp. 157–176.
232. Loppini, A.; Gizzi, A.; Ruiz-Baier, R.; Cherubini, C.; Fenton, F.H.; Filippi, S. Competing mechanisms of stress-assisted diffusivity and stretch-activated currents in cardiac electromechanics. *Front. Physiol.* **2018**, *9*, 1714. [CrossRef]
233. Ruiz Baier, R.; Gizzi, A.; Loppini, A.; Cherubini, C.; Filippi, S. Modelling thermo–electro-mechanical effects in orthotropic cardiac tissue. *Commun. Comput. Phys.* **2019**, *27*, 87–115. [CrossRef]
234. Nicoletti, M.; Loppini, A.; Chiodo, L.; Folli, V.; Ruocco, G.; Filippi, S. Biophysical modeling of *C. elegans* neurons: Single ion currents and whole-cell dynamics of AWCon and RMD. *PLoS ONE* **2019**, *14*, e0218738. [CrossRef] [PubMed]